KAPL, Inc.
Knolls Atomic Power Laboratory
Schenectady, N.Y. 12020-2817
Facsimile (518) 884-1005

LOCKHEED MARTIN

To: The Manager
Schenectady Naval Reactors Office
United States Department of Energy
Schenectady, New York

From: Space Materials

Subject: Assessing the Effects of Radiation Damage on Ni-base Alloys for the Prometheus Space Reactor System (for information only)

Reference: MDO-723-0010, Summary of Structural Materials Considered for the Prometheus Space Nuclear Power Plant (SNPP), January 2006.

Enclosure: Evaluating the Effects of Radiation Damage on Ni-base Alloys for Prometheus.

Attachment: Evaluating the Effects of Composition and Microstructure Evolution on the Radiation-Induced Embrittlement of Candidate Prometheus Pressure Vessel Materials at HFIR

Dear Sir:

This letter provides, for information, a review of the effects of radiation damage on nickel-base alloys to support pre-conceptual Prometheus-1 design efforts.

Summary

Ni-base alloys were considered for the Prometheus space reactor pressure vessel with operational parameters of ~900 K for 15 years and fluences up to 160×10^{20} n/cm^2 (E>0.1 MeV). This paper reviews the effects of irradiation on the behavior of Ni-base alloys and shows that radiation-induced swelling and creep are minor considerations compared to significant embrittlement with neutron exposure. While the mechanism responsible for radiation-induced embrittlement is not fully understood, it is likely a combination of helium embrittlement and solute segregation that can be highly dependent on the alloy composition and exposure conditions. Transmutation calculations show that detrimental helium levels would be expected at the end of life for the inner safety rod vessel (thimble) and possibly the outer pressure vessel, primarily from high energy (E>1 MeV) n,α reactions with ^{58}Ni. Helium from ^{10}B is significant only for the outer vessel due to the proximity of the outer vessel to the BeO control elements. Recommendations for further assessments of the material behavior and methods to minimize the effects of radiation damage through alloy design are provided.

Knolls Atomic Power Laboratory
is operated for the U.S. Department of Energy
by KAPL, Inc., a Lockheed Martin company

Background

Project Prometheus was initiated to develop a space nuclear/electric reactor system for a wide range of deep space and land-based missions. The basic concept selected was a compact fast reactor coupled with a direct gas Brayton cycle turbine that would drive on-board generators for electrical power. The Jupiter Icy Moon Orbiter (JIMO) mission was selected as the first mission and required operation for up to 15 years. The involvement of the Naval Reactor Prime Contractor Team (NRPCT) with this program was terminated in September of 2005 due to a shift in priorities at NASA. The following is a summary of efforts to identify a Ni-base alloy for use as the reactor pressure vessel. From an engineering perspective, a primary concern was containing the pressurized helium-xenon coolant / working fluid. From a materials perspective, the primary concerns were:

- thermal creep,
- microstructural phase stability,
- corrosion in impure helium,
- joining, and
- radiation-induced embrittlement.

All of these issues were addressed in several NRPCT reports and summarized in reference 1. This current report assesses only the radiation-induced embrittlement of Ni-base alloys.

Ni-base and refractory metal alloys were both considered for the pressure vessel as conventional austenitic, ferritic and martensitic steels do not have sufficient thermal creep resistance to meet the design criteria of less than 1% strain at 900 K, 70 MPa for 130,000 hours. Design trade studies favored Ni-base alloys for two main reasons, both related to the concern over a single point failure in the pressurized working fluid loop. First, refractory metal alloys are susceptible to radiation-induced hardening and embrittlement at temperatures below ~0.3 of the melting point or 800 to 1100 K. Second, a dissimilar metal joint between a refractory metal alloy and a conventional alloy plant component would be very challenging due to the propensity for a reduction in the joint ductility due to intermetallic formation. Due to these concerns, the base concept design recommended the use of a Ni-base alloy pressure vessel, eliminating the dissimilar metal joint concern. However, many studies have shown that Ni-base alloys are also susceptible to radiation-induced embrittlement. For the JIMO mission, the expected neutron fluences are generally lower than those investigated in previous studies. Encouragement for using Ni-base alloys was provided by the successful use of Nimonic PE16 as fuel cladding for the Dounreay Prototype Fast Reactor (PFR) in the UK. However, there are very limited neutron irradiation data for the solid solution strengthened alloys considered, Alloys 617 and 230 and Hastelloy X.

Radiation-Induced Swelling

For the JIMO mission, design considerations limited the allowable swelling to 1% swelling. In general, Ni-base alloys have low swelling and were believed to be able to meet this limit. In the 1970s, the United States National Cladding/Duct Materials Development Program screened many commercial alloys for radiation-induced swelling. In these experiments, a minimum in the swelling behavior was reported at nickel contents between 40 and 50 weight percent. Based on these and similar results from other studies, it can be expected that PE16 would exhibit acceptable swelling behavior for the JIMO vessel application. Swelling studies on Hastelloy X indicated that more swelling can be expected than for PE16, but the swelling should be less than one percent allowed for the JIMO mission. Based on these data, low swelling is expected from Alloys 617 and 230, but experimental verification is required.

Irradiation Creep

Creep is a primary concern for JIMO structural materials due to long exposures at elevated temperatures. While thermal creep data for Ni-base alloys is fairly extensive, irradiation creep data are relatively sparse and thus less understood. The irradiation creep behavior of Nimonic PE16 and Hastelloy X were previously evaluated using in-pile creep and post-irradiation tensile creep experiments. Although the results from these results are mixed, none of these show that radiation significantly influenced the creep behavior for the reported conditions. In-pile creep data are superior to post-irradiation data as in-pile results are much more representative of service conditions.

Radiation-Induced Embrittlement

Embrittlement due to irradiation is a major concern for this application. For Ni-base alloys, radiation-induced embrittlement is well known, but quantification is lacking. At very high temperatures ($T>0.5T_m$), embrittlement has been attributed primarily to the formation of grain boundary helium gas bubbles. At lower temperatures (0.3 to $0.6T_m$), both helium and radiation-induced solute segregation are believed to contribute. Helium is produced in Ni-base alloys by high energy (fast) neutron reactions with all Fe, Cr and Ni isotopes and two reactions, with ^{10}B and ^{59}Ni, that respond to low (thermal) energy neutrons. Helium is believed to embrittle grain boundaries by reducing the energy for the nucleation and growth of grain boundary voids. However, very limited work has been reported to correlate the mechanical properties to helium generation and predictions of the mechanical properties are not yet possible. This situation is further complicated by the complex effects of radiation-induced solute segregation and grain boundary precipitation.

Predicted Helium Generation and Embrittlement of the Prometheus Reactor Vessel

To better understand the susceptibility to helium embrittlement, transmutation calculations were conducted to determine the amount of helium produced in the candidate pressure vessel material Alloy 617 as a function of the natural boron content and exposure time for the JIMO mission. The calculations assumed a refractory metal alloy monolithic block core with an Alloy 617 pressure vessel operated for 15 years at 1 MW thermal. The amount of helium produced from ^{10}B was calculated at 50 wppm (~270 appm) natural boron and scaled to the other boron levels of interest. Calculations were made using the RACER Monte Carlo Reactor Physics Code with program inputs of atomic specie, number density, neutron cross section, flux (power/time) and position.

The results show that the energy spectrum is mixed and that the flux is highly dependent on the location in the vessel, Figure 1. Since the control elements are located near the outer vessel, the flux in this region contains more low energy neutrons than for the inner vessel. These inhomogeneities in the energy flux distribution are responsible for variations in helium production. The highest reaction rates are for ^{58}Ni because there are many more ^{58}Ni (60 weight %) atoms than ^{10}B atoms (50 wppm). Integrating the reaction rate data with respect to time produced atomic ppm helium as a function of time and location, Figure 2. At the end of life, the inner vessel region would be expected to produce up to approximately 20 appm helium with the outer vessel region around 10 appm. As the ^{10}B content decreased from 50 wppm to 0 wppm, the amount of helium produced was not significantly reduced for the inner vessel because most of helium would be generated from ^{58}Ni and ^{60}Ni reactions. For the middle of the

outer vessel, this reduction in boron decreased the end of life helium from 10 to ~6 appm, reflecting the 4 appm contribution from ^{10}B (n,α) reactions.

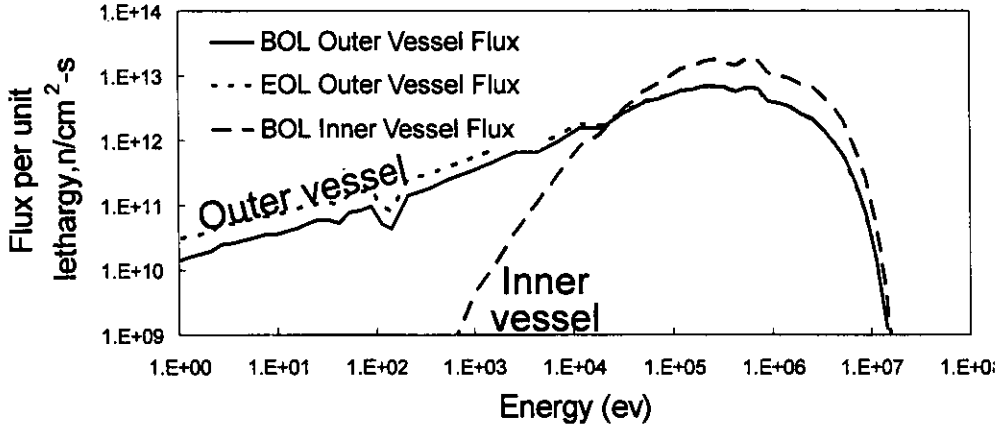

Figure 1 The flux for the JIMO mission would have been a mixed energy spectrum that is highly dependent on the location in the vessel.

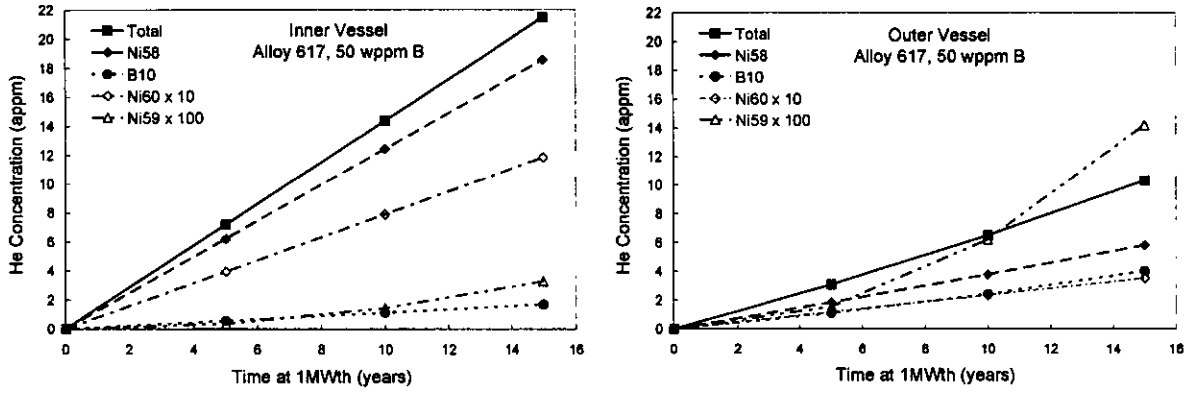

(a) inner vessel for safety rod (thimble) (b) outer vessel.

Figure 2 Calculations showing the amount of helium generated in Alloy 671 containing 50 wppm of natural boron for various isotopes as a function of operational years. (a) inner vessel for safety rod (thimble) and (b) outer vessel. The values shown for ^{59}Ni and ^{60}Ni are multiplied by 100 and 10, respectively.

Correlations between helium and the mechanical properties of Ni-base alloys are very limited as most studies have either focused on correlating helium with swelling or determining fluence and temperature effects on mechanical properties. A systematic study investigating helium and mechanical properties is lacking, although 10 appm helium has been associated with the embrittlement of stainless steel alloys above 773 K.

Mitigation of Radiation-Induced Embrittlement

Methods to reduce the effects of irradiation on the high temperature properties of Ni-base alloys have been proposed and investigated previously. These approaches have included removing ^{10}B, reducing the grain size, reducing the grain boundary tensile stress, retaining helium within

the grains via precipitates (trapping sites), increasing the surface energy to form a void, using grain boundary precipitates to inhibit grain boundary sliding and conducting thermal mechanical treatments prior to irradiation. Examples of studies to explore these remedial methods are briefly reviewed in the Enclosure.

Recommendations for Mitigating Radiation-Induced Embrittlement of Prometheus Vessel

Nickel-base alloys were not designed for neutron exposure at elevated temperatures, therefore the development of nuclear grade materials is warranted. The removal of ^{10}B is evident as a control measure, either by reducing all boron or only ^{10}B. The removal of nickel is more of an academic consideration unless cobalt-based alloys are pursued. Solute segregation can be reduced by lowering the levels of Al, Nb, Ti and Si as well as keeping metalloids very low. Nuclear grade alloy versions would be within the current alloy specifications while reducing elements believed to be responsible for helium embrittlement (i.e., boron) and solute segregation (i.e., Al, Si, Ti). Low grade versions would be below the current specifications. Experiments would be needed to determine the mechanical properties and thermal stability of these developmental alloys. Several radiation studies were planned, but were abandoned when the program was restructured (see Attachment).

Conclusions

Radiation damage was a major concern for Ni-base structural materials considered for the JIMO mission. A literature review and helium transmutation calculations revealed the following:

1. Ni-base alloys are significantly embrittled after neutron exposure at elevated temperatures. This embrittlement has been attributed to a combination of helium and second phase precipitation at grain boundaries.
2. Experimental studies are required to assess radiation-induced embrittlement under prototypical conditions.
3. Radiation-induced swelling and creep would not be expected to exceed design allowables of 1% each.
4. It is strongly recommended that nuclear grade Ni-base and cobalt-based alloys be pursued as a method to mitigate radiation-induced embrittlement by reducing helium generation and solute segregation.
5. Alternative designs to the inner safety rod pressure vessel (thimble) need to be seriously pursued as the current understanding indicates that a Ni-base alloy thimble may be significantly embrittled by radiation.

Significance to NR

This letter summarized the radiation damage concerns for using Ni-base alloys under neutron exposure for the Jupiter Icy Moon Orbiter mission. These concerns are broadly applicable to Ni-base alloys exposed to neutron irradiation, especially at elevated temperatures.

Future Actions

There are no future actions required.

Acknowledgements

The author appreciates the helium transmutation calculations conducted by Jonathan Witter and John Ward at the Knolls Atomic Power Laboratory and technical discussions with George Young, Martin Becker and Matt Frederick at Knolls Atomic Power Laboratory, Erik Mader at Bettis Atomic Power Laboratory and Steve Zinkle at Oak Ridge National Laboratory.

Sincerely,

Tom Angeliu

Tom Angeliu, Principal Engineer
Space Structural Materials
Space Materials/MDO

Approved by:

Youssef Ballout, Manager
Space Structural Materials
Space Materials/MDO

Enclosure 1 to
MDO-723-0043

Assessing the Effects of Radiation Damage on Ni-base Alloys for the Prometheus Space Reactor System

Evaluating the Effects of Radiation Damage on Ni-base Alloys for Prometheus

Author:
Tom Angeliu

With Contributions By:
John Ward
Jonathan Witter

1. Introduction

Project Prometheus was initiated to develop a space nuclear/electric reactor system for a wide range of deep space and land-based missions. The basic concept was a compact fast reactor coupled with a direct Brayton cycle turbine that would drive on-board generators for electrical power, Figures 1 and 2. The Jupiter Icy Moon Orbiter (JIMO) mission was selected as the first mission and required operation for up to 15 years. The involvement of the Naval Reactor Prime Contractor Team (NRPCT) was terminated in September of 2005 due to a shift in priorities at NASA. The following is a summary of the efforts towards identifying a Ni-base alloy for use as the reactor pressure vessel with preliminary design considerations listed in Table 1. From an engineering perspective, a primary concern for this vessel was containing the pressurized helium-xenon coolant / working fluid. From a materials perspective, the primary concerns were:

- thermal creep,
- microstructural phase stability,
- corrosion in impure helium,
- joining, and
- radiation-induced embrittlement.

All of these issues were addressed in several NRPCT reports and summarized in reference 1. This current report primarily assesses the radiation-induced embrittlement of Ni-base alloys.

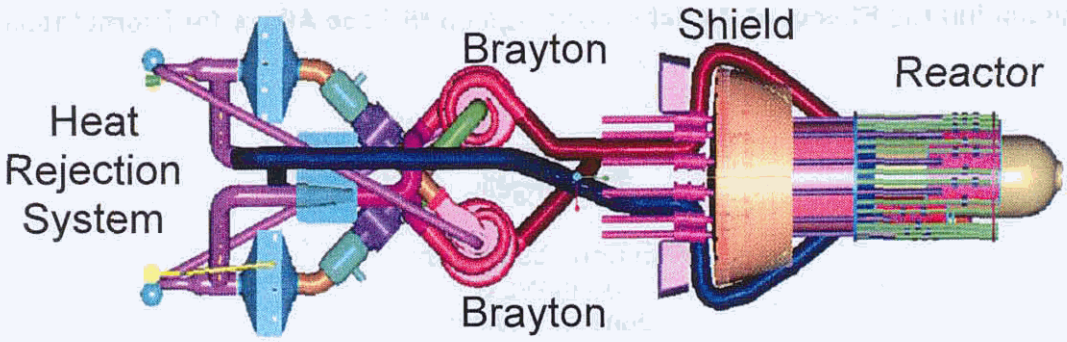

Figure 1 Integrated layout of pre-conceptual Prometheus reactor power system for the Jupiter Icy Moon Orbiter mission.

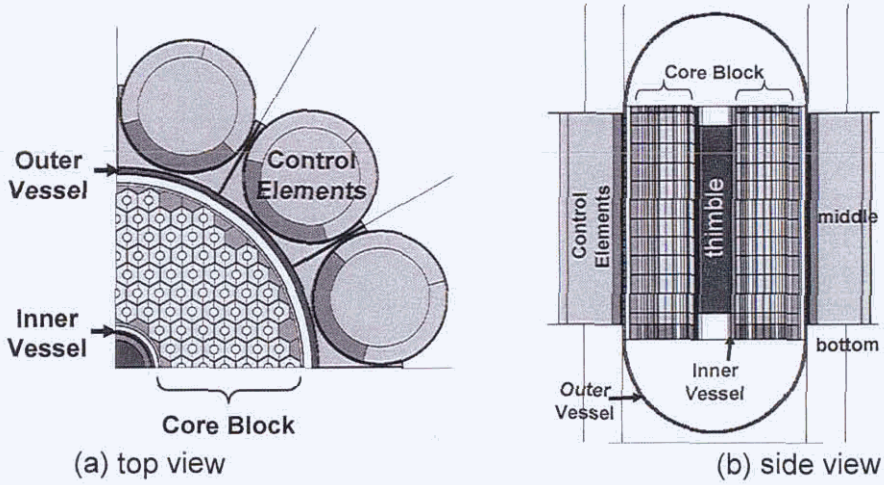

Figure 2 Details from a schematic cross section of a pre-conceptual Prometheus reactor core geometry for the Jupiter Icy Moon Orbiter mission.

Table 1 Preliminary Considerations for One Design of the Prometheus Pressure Vessel.

Temperature Outer Vessel	900 K (other designs are hotter)
Temperature Inner Thimble	To be determined (<1050 K)
Temperature Hot Gas Leg	~1150 K
Stress	70 MPa
Ductility	>1%, primarily for lift off, but a concern for ground test unit cycling
Toughness	Needs to be determined
Creep Strain	<1% in 15 years
Fluence Outer Vessel	$<80 \times 10^{20}$ n/cm^2 (E>0.1 MeV)
Fluence Inner Thimble	$<160 \times 10^{20}$ n/cm^2 (E>0.1 MeV)
Environment	Outer diameter; space vacuum Inner diameter; He/Xe with impurities
Other	Mass (~8 mm thick wall), Neutronics

Ni-base and refractory metal alloys were both considered for the pressure vessel as conventional austenitic and ferritic/martensitic steels do not have sufficient thermal creep resistance to meet the design criteria of less than 1% strain at 900 K / 70 MPa for 130,000 hours. Design trade studies favored Ni-base alloys for two main reasons, both related to a primary engineering concern over a single point failure in the pressurized working fluid loop that would end the mission. First, refractory metal alloys are susceptible to radiation-induced hardening and embrittlement at temperatures below ~0.3 of the melting point or 800 to 1100 K. Second, a dissimilar metal joint between a refractory metal alloy and a conventional alloy plant component would be very challenging due to the propensity for intermetallic formation and a reduction in the joint ductility. Due to these concerns, one preliminary design recommended the use of a Ni-base alloy pressure vessel, eliminating the dissimilar metal joint concern. However, many studies have shown that Ni-base alloys are also compromised by radiation-induced damage. From 1974 to 1985, Ni-base alloys were investigated for advanced cladding and duct materials for the United States Liquid Metal Fast Breeder Reactor (LMFBR) [2]. Ni-base alloys were selected on the basis of their swelling resistance, sodium compatibility and high temperature thermal creep strength, coupled with an extensive industrial base for processing, fabrication and joining [3, 4]. Early experiments revealed that Ni-base alloys with greater than about 40% Ni had excellent swelling resistance [5]. However, these materials were susceptible to radiation-induced grain boundary embrittlement. Several embrittlement mechanisms were proposed, including differential strengthening with radiation-induced precipitation of grain boundary phases [6] and the formation of He bubbles on grain boundaries [7]. Due to this embrittlement, Ni-base alloys were abandoned in favor of swelling and embrittlement resistant austenitic and ferritic / martensitic steels [8]. More recently, Ni-base alloys were investigated for fusion reactors as the first wall material. Initial studies revealed that the relatively high levels of neutron damage (>100 displacements per atom (dpa), $>2000 \times 10^{20}$ n/cm^2, E>0.1 MeV) resulted in significant embrittlement, therefore other materials were pursued.

For the JIMO mission, the expected neutron fluences are generally lower than those investigated in the LMFBR and significantly lower than the fusion studies, with a maximum fluence of 160×10^{20} n/cm^2 (~8 dpa), E>0.1 MeV, for the thimble region and 80×10^{20} n/cm^2 or (4 dpa) for the pressure vessel, Figure 2. Encouragement for using Ni-base alloys was provided by the successful use of Nimonic PE16 as fuel cladding for the Dounreay Prototype Fast Reactor (PFR) in the UK [9-11]. This material experienced $>1600 \times 10^{20}$ n/cm^2 (80 dpa) without a single failure at 673 K to 998 K, suggesting that designs are possible despite the well

documented radiation-induced embrittlement. It is likely that the favorable performance was due to the lack of significant stress on this fuel cladding. In addition to the precipitation strengthened PE16, solid solution strengthened Ni-base alloys Hastelloy X, Alloy 617 and Alloy 230 were considered as vessel materials for the Prometheus reactor, Table 2. Ni-base materials highly alloyed with Al and Ti, and thus cast alloys, were not considered despite their superior creep strength due to limited weldability. Solid solution strengthened Alloys 617 and 230 are more recently developed alloys than Hastelloy X and exhibit superior phase stability and mechanical properties, such as creep strength [12, 13]. There are very limited neutron irradiation data for these alloys, none for Alloys 617 and 230 and little for Hastelloy X.

Table 2 The Composition of Commercial Alloys Considered for the Prometheus Pressure Vessel and Recommended Compositions for Nuclear Grade Versions (weight % or wppm)

Alloy	Ni	Cr	Fe	Mo	W	Co	Ti	Al	Mn	C	other
Alloy 617	54	22	-	9	-	12.5	0.3	1.0	-	0.07	
617NG	54	22	-	9	-	12.5	0.3	0.8	0.3	0.08	<1ppmB
617L	54	22	-	9	-	12.5	-	-	0.3	0.08	<1ppmB
Alloy 230	57	22	<3	2	14	<5	-	0.3	0.5	0.10	0.4Si, 0.02La, <0.015B
230NG	61	22	-	2	14	0.5	-	0.2	0.3	0.10	<1ppmB
230L	61	22	-	2	14	0.5	-	-	0.3	0.10	<1ppmB
Nimonic PE16	44	17	33	3.7	-	-	1.2	1.3		0.05	
PE16NG	44	17	33	3.7	-	-	1.2	1.3	-	0.05	<1ppmB
Hastelloy X	47	22	18.5	9	0.6	1.5	-	-	0.5	0.10	0.5Si, <0.008B
Haynes 188	22	22			14	39					

L = L-grade, NG = nuclear grade

The following sections summarize the effects of neutron irradiation on the swelling, creep and mechanical behavior of relevant Ni-base alloys. A summary of the literature reviewed is found in Table 3. This review was not meant to be comprehensive, but illustrative of the major behaviors reported. In general, experimental data were lacking to address design considerations and extensive radiation test programs were required. One program, presented in the attachment, was proposed for Oak Ridge National Lab in a mixed spectrum reactor. Another program, planned for a Japanese test fast reactor (JOYO-1), is detailed in reference 14.

1. Radiation-Induced Swelling

The United States National Cladding/Duct Materials Development Program was initiated for the development of reference and advanced materials for liquid metal fast breeder reactor applications. Initial experiments included the screening of many commercial alloys for radiation-induced swelling. In the first experiment, B-109, thirteen alloys were exposed to a fast spectrum at the Experimental Breeder Reactor-II (EBR-II). A second experiment (AA-1) narrowed this evaluation to six alloys. In these experiments, materials were irradiated to fluences of 1200 to 1500 $x10^{20}$ n/cm^2 (E>0.1 MeV) at temperatures from 673 K to 923 K. A minimum in the swelling behavior was reported at Ni contents between 40 and 50 weight percent, as shown in Figure 3, with PE16 displaying some of the lowest swelling behavior [5]. These initial studies also showed that aging treatments applied to both solution annealed and cold worked alloys increased swelling, but the reason was not fully understood. Additional swelling studies with PE16 in EBR-II produced less than 1% swelling after irradiation between 44 to 77 dpa ($880x10^{20}$ to $1500x10^{20}$ n/cm^2) at 667 to 909 K [7]. Lower swelling was also reported for PE16 containing 25 ppm B rather than 50 ppm B after irradiation in the Dounreay Fast Reactor up to $900x10^{20}$

n/cm^2 (48 dpa) between 673 and 873 K [15, 16]. Based on these results, it can be expected that PE16 would exhibit an acceptable level of swelling in a JIMO vessel application.

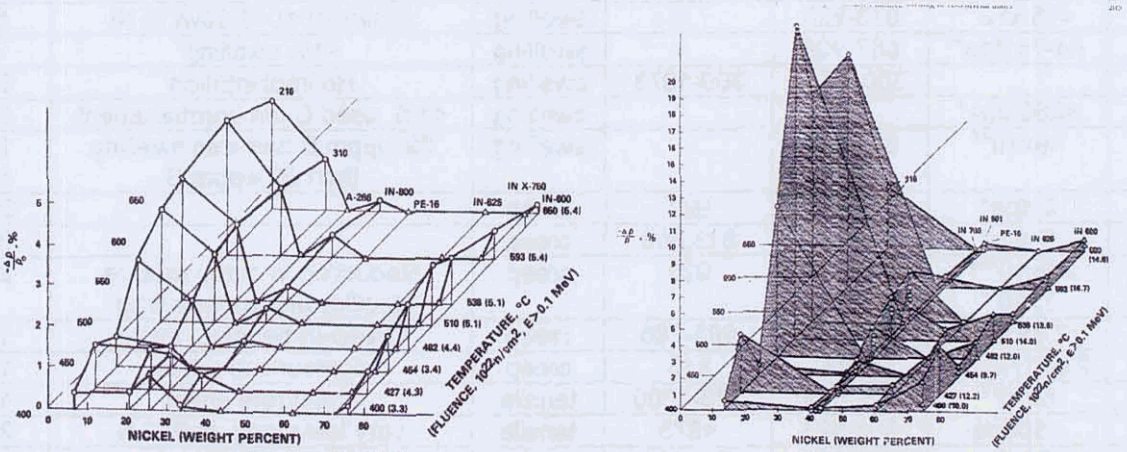

(a) Experiment B-109 (b) Experiment AA-I

Figure 3 Swelling behavior versus the nickel content and temperature for alloys evaluated in the United States National Cladding/Duct Materials Development Program [5]. Notice a minimum in swelling at 40 to 50 wt.% Ni.

Table 3 A literature summary on the effects of neutron irradiation on Ni-base alloys.

Alloy	Fluence (n/cm^2)	Irrad. T (K)	Test T (K)	Property	Comments	Ref
PE16	$<15 \times 10^{22}$	673-923		swelling	minimum at 40-50wt.% Ni	5
PE16	44-74 dpa*	667-909		swelling	<1% swelling	7
PE16		300-1073	300-1073	swelling	He implantation	54
PE16	<280 dpa*	798		swelling	<1%, used C ion bombardment	55
PE16	$<9 \times 10^{22}$	673-873		swelling	29 wppm B had less swelling than 50 wppm B	15 16
PE16	8 dpa*	503-623	923	creep		20
PE16	5 dpa*	823,858	823,858	creep		20
PE16	1.5×10^{19}** 7×10^{18}	318K	923	creep	Reduction in creep rupture ductility and rupture time	24
PE16	7.8×10^{21}	693-785	693-785	creep	Creep-in-bending, insitu	19
PE16	2 to 17×10^{22}	813K	813	creep	pressurized tubes	18
PE16	5×10^{22}	773-1000	773-1000	tensile	strain rate effect	45
PE16	<50dpa	503-623	<973	tensile	very low elong. at 973 K	20
PE16	<20 dpa	823,953	823,953	tensile	low elongations	20
PE16			673-923	tensile	implanted with He and Li	27
PE16	2×10^{20}	318,923	973	tensile	low ductility	56
PE16	$12\text{-}40 \times 10^{21}$	650-823	683-973	tensile	Effect of heat treat, includes swelling effects	40
PE16	2×10^{22} 5×10^{22}	723-898	698-1008	tensile	ductility decrease attributed to gamma prime on grain boundaries	41
PE16	$2,5,7 \times 10^{22}$	400-1008	823-973	tensile	ductility trough of near zero ductility after irrad.	6
PE16	20-29 dpa	748,823, 923	748,823, 923	tensile	low B increases ductility from 0.1% to 1.5 to 2.0%	20
PE16	5.7×10^{22}	738-850	783-933	ring test	much reduced ductility, lowest at 823 K	57
Hast X	5×10^{22}	873-923	873-923	swelling	relates swelling to precipitate microstructure	17
Hast X	**	923	923	creep	decreased rupture strength	23
Hast X		889-944	889-944	creep	no fluence reported	21
Hast X	6.6×10^{20}**		1173	creep	irradiation increased the creep strength	33
Hast X	1.1×10^{22}	923	823-1123	tensile	elongations >1%, no change in yield, strain rate	46
Hast X	3.3×10^{20}	811	856,977	tensile	Includes Alloys 625, 800	28
Hast X	3.3×10^{20}	299, 866, 977	300	tensile	reduced ductility at all T, hardening at 299 K & 866 K	27
Hast X	1.1×10^{21}**	648	873-1123	tensile	good ductility at elevated temperature testing	27
Hast X	10^{20}-10^{21}**		873-1273	tensile	low B (<0.2 wppm) retains high ductility (28%)	27
Hast X	$<2 \times 10^{21}$**		1173, 1273	tensile	~10X reduction in tensile ductility	35
Hast X-280	2.5×10^{19} 1.2×10^{21}	973	300, 923	tensile	low Co Hast X, % elong. 48% to 25% and 5% after irrad.	58

*1 dpa is approximately 20×10^{20} n/cm^2 for Ni-based alloys [15]
**denotes thermal neutrons, otherwise all fluences were fast

Swelling studies on solid solution strengthened Ni-base alloys have focused on Alloy 625, Hastelloy X and Alloy 800. These materials produced <0.6%, 0.6 to 2.1% and 0.5 to 5% swelling, respectively after exposure in EBR-II to $500x10^{20}$ n/cm^2 at 873 to 923 K [17]. The variation in the swelling behavior was attributed to the precipitate microstructure. The Ni-base Alloy 800 has no second phase strengtheners and swells similar to 304SS. Alloy 625 swelled the least because it has much finer, semi-coherent gamma double prime precipitates that are believed to lower the overall point defect concentration by providing sites for annihilation of vacancies and interstitials. Likewise, the swelling resistance of PE16 has been attributed to the presence of fine, coherent precipitates of gamma-prime. This analysis suggests that more swelling can be expected in Hastelloy X than PE16, but the values should be less than one percent for the JIMO mission. It is more difficult to predict the amount of swelling for Alloys 617 and 230 since no radiation data have been found. Alloy 617 contains sufficient aluminum to form gamma prime and could be expected to behave like PE16 since the aluminum contents are similar. Alloy 230 precipitates a homogeneous distribution of carbides during thermal exposure, which may produce swelling behavior similar to Hastelloy X. The EBR-II study demonstrated adequate swelling resistance for Hastelloy X (0.6 to 2.1%) at $500x10^{20}$ n/cm^2 and at temperatures relevant to the JIMO application. This suggests that at mission fluences up to $160x10^{20}$ n/cm^2, the related Alloys of 617 and 230 may have adequate swelling resistance. However, swelling data must be obtained before committing these materials to an actual design.

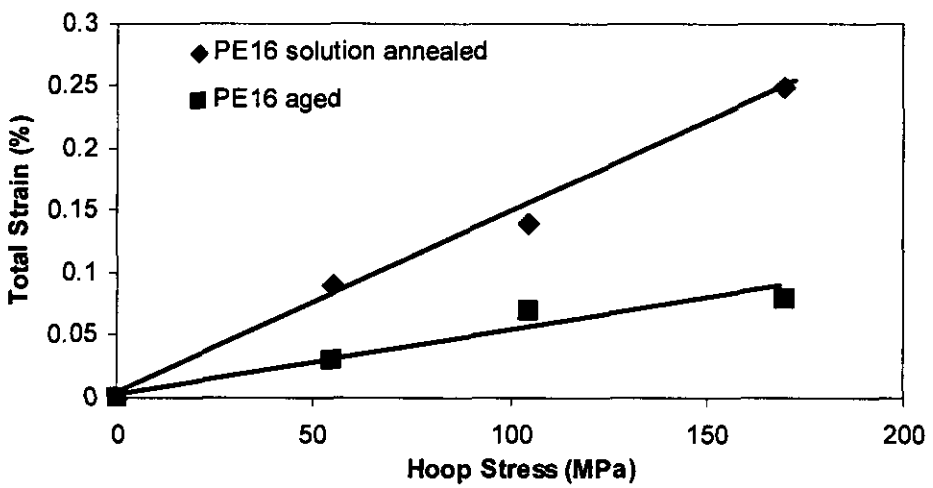

Figure 4 The total strain as a function of hoop stress for PE16 in the solution annealed (ST, 1353 K/4hr) and solution annealed + aged (STA, ST + 1173 K/1hr + 1023 K/8hr) conditions after irradiation at approximately 813 K at fluences of 200 and $400x10^{20}$ n/cm^2 (E>0.1 MeV) in EBR-II [18].

2. Irradiation Creep

The irradiation creep behavior of Nimonic PE16 and Hastelloy X were previously evaluated using in-pile creep and post-irradiation tensile creep experiments. Biaxial creep specimens of PE16 were irradiated at approximately 813 K at fluences of 200 and $400x10^{20}$ n/cm^2 (E>0.1 MeV) in EBR-II [18]. Four pressurized tubes of each PE16 heat treat condition were studied, one at zero stress and the others at the three stresses of 55, 110 and 170 MPa. Figure 4 shows the total strain as a function of hoop stress for PE16 in the solution annealed (ST) and solution annealed + aged (STA) conditions. These results show that the total strain in the solution annealed condition does not exceed 0.25% at the highest stress of 170 MPa (24.7 Ksi). This is the total strain, which is a combination of irradiation creep, thermal creep and swelling, thus the

irradiation creep component was no more than 0.25%. An irradiation creep in-bending experiment was conducted for solution annealed and aged PE16 in EBR-II. Minimal creep strain was reported after exposures of $48x10^{20}$ n/cm^2 at 755 K (0.03% creep strain) and $72x10^{20}$ n/cm^2 at 693 K (0.11%) [19]. In another investigation, post-irradiation tensile creep of PE16 was conducted after two different irradiation conditions at the Dounreay Fast Reactor [20]. In one condition, PE16 was irradiated to $160x10^{20}$ n/cm^2 (8 dpa) at 503 K to 623 K and then thermally crept at 923 K. These specimens exhibited an increase in the secondary creep rate in the solution annealed and aged conditions relative to unirradiated materials. In another post-irradiation creep experiment, PE16 was irradiated at a lower fluence (5 dpa, $100x10^{20}$ n/cm^2) and higher temperatures (823 K and 858 K) and then crept at the irradiation temperatures. These experiments showed a reduction in the secondary creep rate and increases in the creep rupture strength for the irradiated material. Although the results from these published results are mixed, none of these results show that radiation significantly influenced the creep behavior for the reported conditions. In-pile creep data is far superior to post-irradiation data as in-pile results are much more representative of in service conditions. The JOYO-1 test matrix was intended to provide in-pile creep data from a fast spectrum reactor [14].

Hastelloy X was also evaluated using biaxial stress-rupture specimens as part of a fuel cladding evaluation for a space power reactor, Irradiation Experiment NAS-120 [21]. Unirradiated and irradiated specimens were crept at 922 K and 977 K. All of the irradiated specimens ruptured in less than about 600 hours, even at the lowest stress levels of 132 MPa at 922 K and 101 MPa at 977 K, Table 4. Unfortunately, no creep strain data or irradiation conditions were reported. The most significant result was that the irradiated creep rupture ductility of Hastelloy X was less than 2.1%. Unirradiated creep rupture data were not reported, but creep rupture strain for Hastelloy X can exceed 40% at 1033 K and 100 MPa [22]. In another experiment, post-irradiation creep studies on Hastelloy X reported a decrease in the stress rupture strength after thermal neutron irradiation to $0.5x10^{20}$ n/cm^2 at 923 K [23]. A small difference in the minimum creep rate of Hastelloy X was reported after exposure to irradiation at 889 K to 944 K in excess of 13,000 hours in the Hanford Reactor [21]. As with PE16, these limited data suggest that radiation does not significantly influence the creep strain, however, the creep rupture ductility was significantly reduced.

Table 4 Irradiated Hastelloy X Biaxial Creep Data (Heat C6505) [21]

Test Temp (K)	Irradiation Temp (K)	Stress (Ksi)	Stress (MPa)	Rupture Time (hr)	Rupture Ductility (%)
977	899	24.2	167	5.9	NA
977	922	25.5	176	15.6	0.99
977	916	19.0	131	83.8	NA
977	944	14.7	101	607	0.97
922	888	28.7	198	90	2.0
922	888	24.5	169	266	2.1
922	922	18.8	130	573	NA
922	899	19.1	132	511	NA

3. Radiation-Induced Embrittlement

The radiation-induced embrittlement of Ni-base alloys is well known, but quantification based on time, temperature, energy spectrum, flux and composition are lacking [24, 25]. At very high

temperatures ($T>0.5T_m$), embrittlement has been attributed primarily to the formation of grain boundary helium gas bubbles [26]. At lower temperatures (0.3 to $0.6T_m$), both helium and radiation-induced solute segregation are both believed to contribute to embrittlement [25]. Helium is primarily produced in Ni-base alloys by high energy (fast) neutron reactions with all Fe, Cr and Ni isotopes and two reactions that occur throughout the neutron energy spectrum. Natural Ni contains 68% ^{58}Ni and 26% ^{60}Ni, with the fast neutron n,α reactions of

$$^{58}Ni + n_f \rightarrow {}^{55}Fe + {}^{4}He, \quad (1)$$

$$^{60}Ni + n_f \rightarrow {}^{57}Fe + {}^{4}He. \quad (2)$$

The high thermal neutron cross section of ^{10}B, which makes up ~20% of naturally occurring boron, is responsible for significant transmutation at relatively low thermal fluences by the n,α reaction of

$$^{10}B + n \rightarrow {}^{7}Li + {}^{4}He. \quad (3)$$

Systematic experimental studies have shown that Li can also contribute to a loss in ductility, but helium was reported to be a more effective embrittling agent [27]. This is consistent with atomistic modeling results [28, 29]. Helium can also be produced by the two step reaction of

$$^{58}Ni + n \rightarrow {}^{59}Ni + \gamma, \quad {}^{59}Ni + n \rightarrow {}^{56}Fe + {}^{4}He, \quad (4)$$

but this reaction requires production of ^{59}Ni first. Helium generation is very dependent on the energy spectrum, cross section and fluence and has been reported as atomic parts per million (appm) versus fluence for a variety of fast, thermal and mixed spectrums [26, 30-34]. For Ni-base alloys, it has been reported for a thermal neutron dominant reactor that the transmutation of boron to helium dominates at low fluences (to about 10^{20} n/cm^2), while helium from Ni-neutron interactions dominates at high fluences (above 10^{20} n/cm^2) [35]. For a fast reactor environment relevant to the Dounreay Prototype Fast Reactor, the helium production rate was reported to be ~1 appm per dpa for materials exposed up to ~100 dpa [36]. Note that 1 dpa is ~20×10^{20} n/cm^2 [15]. This trend was based on linear estimates for greater than 40 dpa exposures and may not account for low fluence effects depending on the amount of thermal neutrons and ^{10}B [34, 37]. Further calculations at energy spectrums typical of the JIMO design and at lower fluences are provided in Section 5.

Mechanistically, helium is believed to embrittle grain boundaries due to stress enhanced growth of voids by reducing the energy for the nucleation and growth of these grain boundary voids [26]. While this mechanism has been supported by many studies, there are still many unanswered questions about the sensitivity of bubble nucleation and growth with materials and exposure parameters. Very limited work has been reported to correlate the mechanical properties to helium generation. One study on Hastelloy X reported a progressive decrease in the total elongation as a function of thermal neutron dose and increased amount of calculated helium, Table 5, although no microstructural characterization was reported [34]. In general, no predictions of the mechanical properties are yet possible for a given material with a given set of experimental parameters. This situation is further complicated by the complex effects of radiation-induced solute segregation and grain boundary precipitation.

Radiation-induced solute segregation is a non-equilibrium segregation process that occurs at point defect sinks during irradiation between approximately 0.3 to 0.5 of the melting temperature [38]. Radiation produces point defects in excess of thermal equilibrium concentrations. At high temperatures, these defects are mobile and travel to low energy sites such as grain boundaries,

and can interact with solute elements along the way to promote enrichment or depletion at grain boundaries. If the enrichment exceeds the solubility limit, second phases may form. The segregation of impurity elements such as S, P, Sb, As, Sn, etc. are well known to embrittle grain boundaries, especially for steels where increases in the hardness along with impurity segregation act synergistically to lower ductility [39]. Auger analysis of PE16 grain boundaries irradiated in EBR-II revealed slight enrichments of P and S, a release of He upon fracture, changes in the bulk alloying elements and a continuous layer of gamma prime along the grain boundaries [40, 41]. In general, the literature indicates that radiation-induced solute segregation promotes a continuous grain boundary coverage of intermetallic phases that are more detrimental to radiation-induced embrittlement than segregated impurities such as S and P.

Table 5 Effect of Thermal Neutron Dose on the Total Elongation of Hastelloy X Tensile Tested at 0.67% strain / min (~1.1×10^{-4} s^{-1}) After Irradiation [34].

T_{test} (K)	Thermal neutron dose (n/cm^2)	Calculated atom fraction of He	Total Elongation (%)
973	NA	0.04	30
	NA	0.4	20
	NA	4	8
1173	2.7×10^{17}	0.004	50
	2.2×10^{18}	0.04	40
	2.4×10^{19}	0.4	20
	4.3×10^{20}	5	7
	2.0×10^{21}	40	5
1273	2.7×10^{17}	0.004	40
	2.2×10^{18}	0.04	30
	2.4×10^{19}	0.4	6
	4.3×10^{20}	5	4

Mechanistically, continuous grain boundary coverage by intermetallics promotes embrittlement by restricting grain boundary deformation, especially when the matrix becomes hardened [6]. Without sufficient plasticity to accommodate strain, these factors act to promote grain boundary failure at relatively low levels of plastic strain. The literature shows that a continuous layer of γ' can form along the grain boundaries of irradiated, precipitation hardened Ni-base alloys, including solution annealed PE16 and has been associated with significant decreases in ductility [6, 41-43]. For aged PE16, the coverage of γ' on grain boundaries after irradiation is expected to be less pronounced than for solution annealed material and contribute less to embrittlement [7]. Wrought solid-solution strengthened Ni-base alloys that contain little to no elements that form intermetallics (Ti, Nb and Al) and are believed to be less susceptible to this embrittlement. All of the Ni-base alloys considered for JIMO (PE16, Alloy 617 and Alloy 230) contain the intermetallic former Al, while PE16 and Alloy 617 contain Ti and may be susceptible to radiation-induced γ' precipitation on grain boundaries. However, correlations between the Al or Ti contents and embrittling exposure conditions have not been established, so compositional limits cannot be recommended.

4.1 Review of Mechanical Test Data. There has been a significant amount of mechanical testing conducted on irradiated Nimonic PE16 and a lesser amount on other Ni-base alloys of interest, Table 3. The data consistently show that irradiation increases the yield and ultimate tensile strengths with a corresponding decrease in tensile ductility. Only two illustrative studies for PE16 are presented. In the first example, the tensile and yield strengths were determined

for PE16 irradiated at two conditions in the Dounreay Fast Reactor [20]. In one condition, PE16 was irradiated to 20 dpa ($4x10^{22}$ n/cm^2) at 503 K to 623 K and then tested from 573 K to 1023 K. In another irradiated condition, PE16 was irradiated at 823 K and 858 K and tested at the same temperatures. After both exposures, PE16 showed radiation hardening with increased yield strengths, especially at the lower tensile test temperatures. Figure 5 shows the significant increase in the yield strength and decrease in total elongation at 823K and 873K.

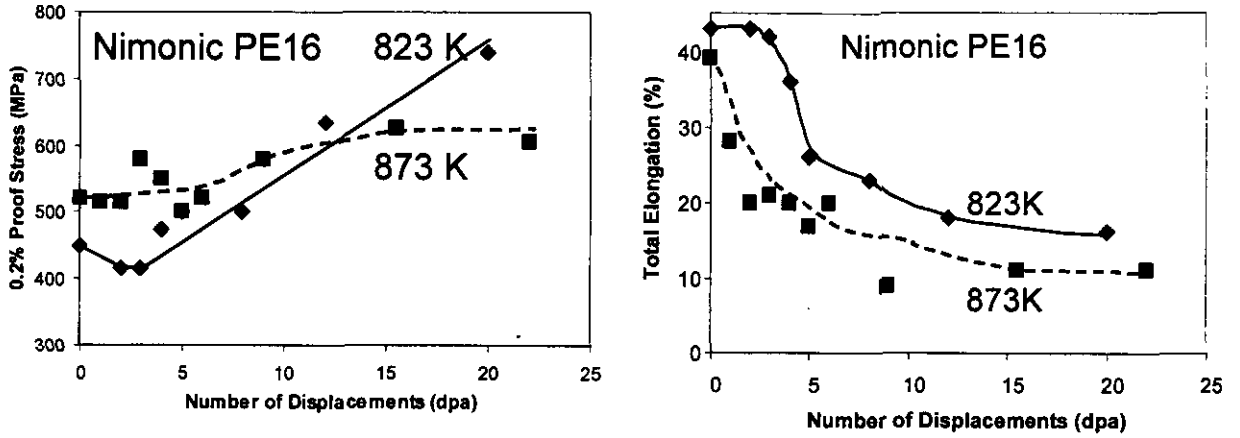

(a) yield strength (b) total elongation

Figure 5 The dependence on damage level of the tensile properties of Nimonic PE16 (heat treatment 3) irradiated and tested at 823 K to 873 K [20].

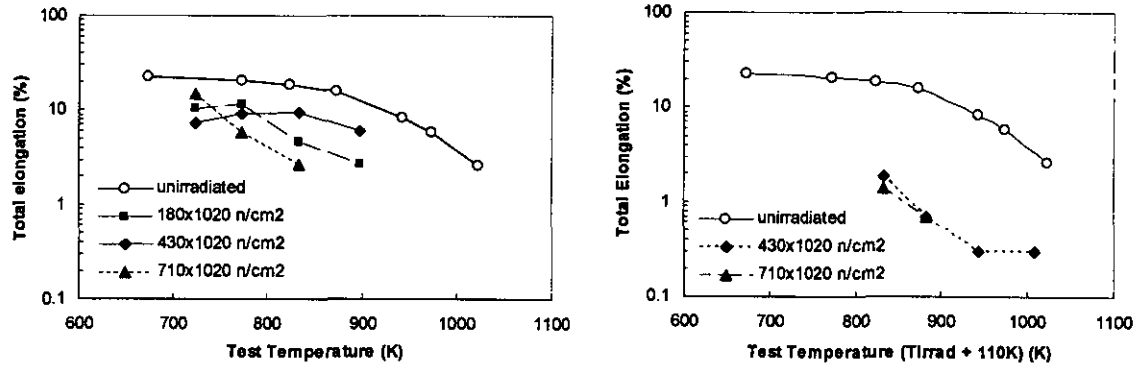

(a) Tested at T_{irrad} (b) Tested at 110K above T_{irrad}

Figure 6 A significant decrease in the total elongation of Nimonic PE16 when tested at (a) the irradiation temperature (T_{irrad}) and (b) 110 K above T_{irrad} [6].

In the second example, solution annealed (not aged) PE16 was irradiated in EBR-II at fluences of 180, 430 and $710x10^{20}$ n/cm^2 at temperatures ranging from 723 K to 1008 K [6]. Tensile specimens were tested at 400 K, representing refueling temperatures for EBR-II, the irradiation temperature and 110 K above the irradiation temperature, representative of a temperature excursion. Tensile testing at 400 K showed significant strengthening after irradiation, but the ductility still exceeded 10% elongation. Tensile testing at the irradiation temperature showed significant increases in the yield strength for test temperatures below 923 K with minimal increases in the tensile strengths. The ductility of these specimens decreased significantly, as

low as 1.5% at 833 K, Figure 6a. When specimens exposed to these same conditions were tensile tested at 110 K above the irradiation temperature, the ductility was reduced even further and in some cases, near zero ductility was observed, Figure 6b. These results were attributed to differential strengthening, or the large difference in the strength of the matrix to that of the grain boundary, resulting in intergranular fracture. In this mechanism, irradiation increases the strength of the matrix to a point where deformation primarily occurs at grain boundaries, resulting in low ductility. The authors argued against grain boundary weakening mechanisms such as He embrittlement and solute segregation, but no direct evidence was provided showing that these mechanisms were not operating. In fact, data used to advocate that helium embrittlement was not applicable were found to be statistically insignificant [44].

For solid solution strengthened Ni-base alloys, the effects of neutron irradiation on the mechanical properties are similar to those reported for precipitation hardened alloys. The yield and ultimate tensile stresses are increased and the elongation to failure is decreased. Figure 7 illustrates this for Hastelloy X exposed to 3.3×10^{20} n/cm^2 at temperatures of 299 K, 866 K and 997 K [23]. Tables 5 and 6 show significant decreases in the tensile ductility of Hastelloy X with thermal and fast neutron exposure, respectively [28, 32]. The fast neutron exposed materials exhibited brittle grain boundary failure while the unirradiated specimens displayed ductile transgranular failure. No microstructural characterization was conducted to assess the effects of radiation-induced segregation and precipitation, although thermal aging did decrease the ductility, Table 6.

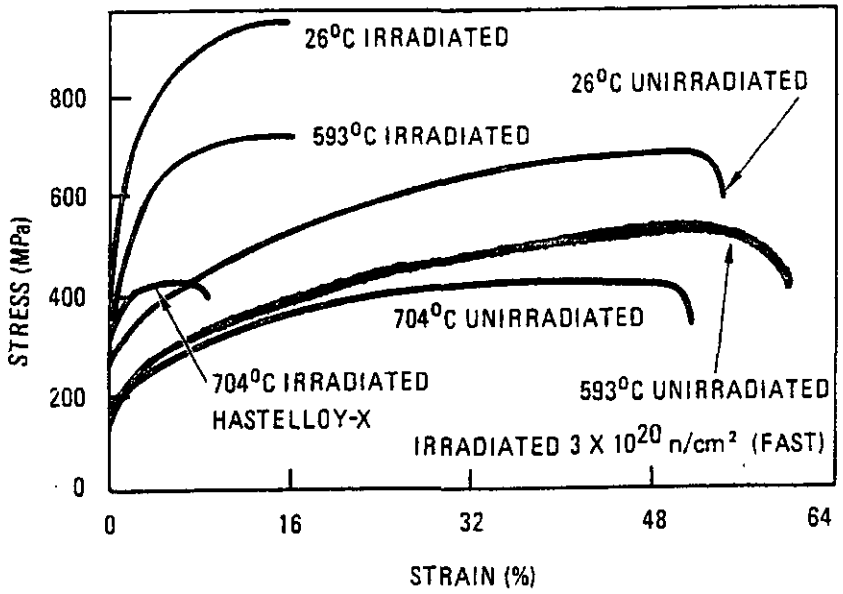

Figure 7 Stress-strain curves for Hastelloy X before and fast neutron irradiation at 3.3×10^{20} n/cm^2 [23].

The strain rate is important to the mechanical behavior, as lower strain rates produced lower ductilities for both precipitation hardened and solid solution strengthened Ni-base alloys. For solution annealed and aged PE16 irradiated to ~500×10^{20} n/cm^2 in EBR-II, a decrease in the strain rate by two orders of magnitude reduced the total elongation up to a factor of 10, Table 7 [45]. For Hastelloy X irradiated to 110×10^{20} n/cm^2 in a mixed spectrum reactor (BR 2 in Belgium), the loss in ductility was more severe as the test strain rate decreased and the temperature increased, Table 8 [46]. Unfortunately, unirradiated materials were not tested for comparison, therefore it is difficult to assess how much of this behavior is attributed to irradiation

and how much to creep. One study on Hastelloy X showed similar decreases in ductility as a function of strain rate for irradiated and unirradiated material [34]. If helium were enhancing grain boundary voiding, then slower strain rates would allow more time for helium diffusion and creep damage to accumulate at grain boundaries to produce intergranular fracture morphology. Limited creep rupture data for irradiated Hastelloy X illustrate the extent of creep rupture ductility loss, Table 4, but no comparison was made to unirradiated, thermally aged material to determine if this effect was due to irradiation or thermal aging [21]. Experiments and modeling of PE16 indicate that low failure strains are a result of closely spaced voids at grain boundary helium bubbles [36]. At low stresses, the rupture life of irradiated Ni-base alloys may be determined by the rate of gas-driven bubble growth rather than by their unirradiated creep strength.

Table 6 Effect of Fast Neutron Irradiation on the Tensile Properties of Hastelloy X Before and After Exposure in EBR-II at/or aged at 856 K for 200 hours [30].

T_{test} (K)	Strain Rate (min^{-1})	Fast neutron (n/cm^2)	Yield Stress (MPa)	UTS (MPa)	Uniform Elongation (%)	Total Elongation (%)
299	0.02	None	300	863	50	54
299	0.02	None - aged	308	724	44	47
299	0.02	$3.3x10^{20}$	450	945	16	16
856	0.02	None	183	661	55	57
856	0.02	None - aged	223	609	44	46
856	0.02	$3.3x10^{20}$	361	709	14	15
977	0.02	None	184	425	41	50
977	0.02	None - aged	181	414	26	35
977	0.02	$3.3x10^{20}$	333	427	5.4	8.4

Table 7 Effect of Tensile Strain Rate on the Ductility of Neutron Irradiated PE16 (solution annealed and aged) Tested at Tirrad + 110 K [45].

Specimen number	T_{irrad} (K)	T_{test} (K)	Strain rate	Yield (MPa)	UTS (MPa)	% Uniform Elongation	% Total Elongation
H12	773	883	$4x10^{-2}$ s^{-1}	717	830	5.5	5.5
H29	773	883	$4x10^{-4}$ s^{-1}	749	770	0.7	0.7
H37	833	943	$4x10^{-2}$ s^{-1}	634	726	3.5	3.5
H42	833	943	$4x10^{-4}$ s^{-1}	644	652	0.3	0.3
H103	898	1008	$4x10^{-2}$ s^{-1}	661	867	3.3	3.3
H111	898	1008	$4x10^{-4}$ s^{-1}	527	534	0.3	0.3

Table 8 Effect of Tensile Strain Rate on the Ductility of Hastelloy X Irradiated at 923 K [46].

T_{test} (K)	Strain Rate min^{-1}	% Total Elongation	T_{test} (K)	Strain Rate min^{-1}	% Total Elongation	T_{test} (K)	Strain Rate min^{-1}	% Total Elongation
823	5	5	973	5	5.5	1123	5	2
	$1.2x10^{-1}$	5		$1.2x10^{-1}$	5		$1.2x10^{-1}$	1
	$2.4x10^{-3}$	4.5		$2.4x10^{-3}$	4		$2.4x10^{-3}$	0.8
	$5x10^{-6}$	4		$5x10^{-6}$	1.5		$1x10^{-6}$	0.3

4. Predicted Helium Generation and Embrittlement of the Prometheus Reactor Vessel

Based on prior studies summarized in Section 4, radiation-induced embrittlement appears to be a major concern, but critical parameters such as fluence, temperature, composition and ductility vs. appm He are not understood well enough to be specified. To better understand the susceptibility to helium embrittlement, transmutation calculations were conducted to determine the amount of helium produced in the candidate pressure vessel material Alloy 617 as a function of the natural boron content and exposure time for the JIMO mission. The calculations assumed a refractory metal alloy monolithic block core concept with an Alloy 617 pressure vessel operated for 15 years at 1 MW of thermal power. The amount of helium produced from ^{10}B was calculated at 50 wppm (~270 appm) natural boron and scaled to the other boron levels of interest. Helium transmutation calculations were made using the RACER Monte Carlo Reactor Physics Code [47]. The program inputs included the geometry, atomic specie, number density, neutron cross section, flux (power/time) and control position.

The results show that the energy spectrum is mixed and that the flux is highly dependent on the location in the vessel, Figure 8. Over the entire energy spectrum, the peak flux for the inner vessel (i.e. thimble) is higher than the outer vessel. However, since the control elements are located near the outer vessel, the flux in this region contains more low energy neutrons than for the inner vessel. With operation, a change in the control element position from the beginning of life (BOL) to end of life (EOL) has a significant effect on the lower energy flux. These inhomogeneities in the energy flux distribution are responsible for variations in the production of helium. By considering the flux and neutron cross sections, the n,alpha reaction rates for ^{10}B and ^{58}Ni are calculated and summarized in Figure 9. The highest reaction rates are for ^{58}Ni because there are many more ^{58}Ni (60 wt. %) atoms than ^{10}B atoms (50 wppm). Figure 9 also shows that the reaction rate for ^{10}B increases slightly as the energy decreases, despite the lower fluxes at lower energies shown in Figure 8. This may be explained by increases in the neutron cross section of ^{10}B as the energy decreases, which leads to higher reaction rates. These results illustrate the importance of analyzing the reaction rates with respect to energy spectrum resolution as it would otherwise be difficult to relate helium production to fluence in the traditional sense of total, thermal neutrons E<0.1 MeV, or fast neutrons E>1.0 MeV, as typically presented in the literature.

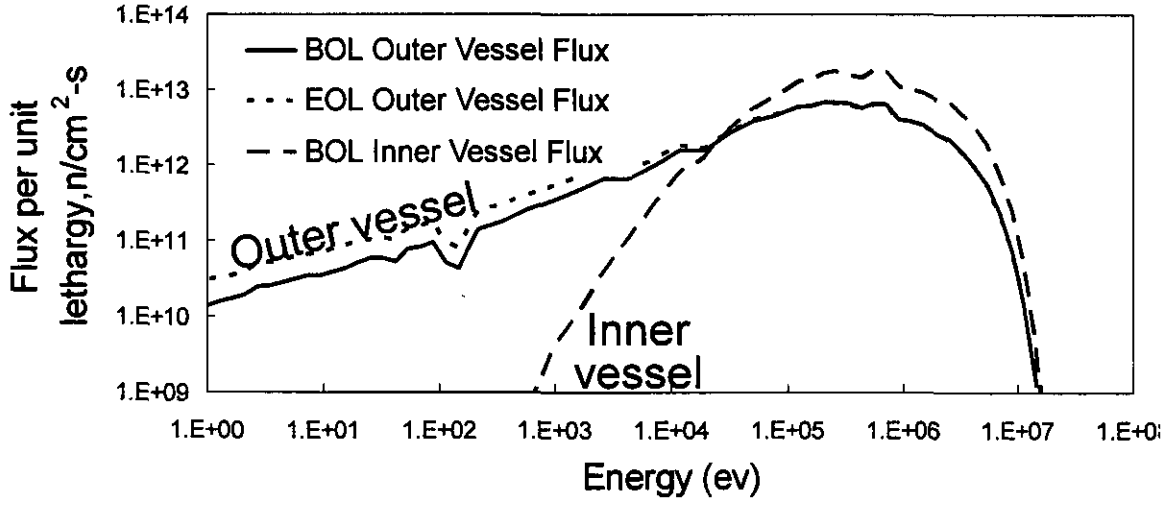

Figure 8 The flux for the JIMO mission would have been a mixed energy spectrum that is highly dependent on the location in the vessel.

Integrating the area underneath the curves in Figure 9 with respect to time produced the results shown in Table 9. By the end of life, the inner vessel region would be expected to produce up to approximately 20 appm helium while the outer vessel region would be expected to produce up to approximately 10 appm. As the ^{10}B content decreased from 50 wppm to 0 wppm, the transmutated helium was not significantly reduced for the inner vessel because most of the helium is generated from ^{58}Ni and ^{60}Ni reactions. For the middle of the outer vessel, a reduction in boron from 50 to 0 wppm decreased the end of life helium from 10 to ~6 appm, reflected the almost 4 appm contribution from ^{10}B (n,α) reactions. Additional details for the helium production as a function of operational time and isotope are shown in Figures 7a and 7b, for the inner vessel and outer vessel, respectively. These figures show that the production of helium from ^{58}Ni, ^{60}Ni and ^{10}B is essentially linear with time, with an incubation period observed for helium produced from the two step $^{58}Ni/^{59}Ni$ reaction as expected. This incubation period is more noticeable for the outer vessel, Figure 7b, due to the larger flux of thermal neutrons. Since the amount of helium produced from ^{10}B is not saturated with time, not all of the ^{10}B has been converted to ^{7}Li and ^{4}He.

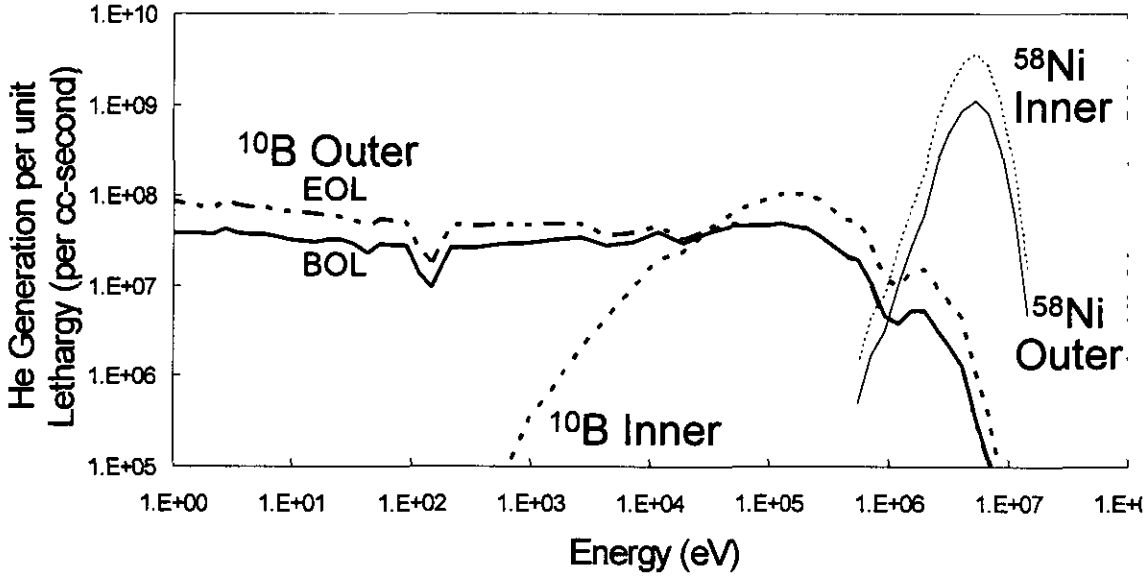

Figure 9 The (n, alpha) ^{10}B and ^{59}Ni reactions are non-threshold reactions while the ^{58}Ni reaction requires a threshold energy of about 1 MeV to occur.

Table 9 Calculated Helium (appm) Production for Alloy 617 at Four Regions in a Proposed Prometheus Reactor Pressure Vessel.

		Contribution % From				
Region	Helium with 50 wppm B	^{58}Ni	^{59}Ni	^{60}Ni	^{10}B	Helium with 0 wppm B
OD, middle	10.3	53.5	0.9	3.4	39.1	6.3
OD, bottom	1.2	59.4	0.1	3.9	33.5	0.8
ID, middle	22.4	82.0	0.2	5.4	7.5	20.7
ID, bottom	5.6	78.0	0.0	5.0	12.4	4.9

OD = outer diameter, ID = inner diameter

Correlations between helium and mechanical properties of Ni-base alloys are very limited as most studies have either focused on correlating helium with swelling or determining fluence and temperature effects on mechanical properties. A systematic study investigating He and mechanical properties is lacking, although 10 appm helium has been associated with the embrittlement of stainless steel alloys above 773 K [48]. The most relevant study reports results from Fe-45Ni-20Cr alloys that were either implanted with helium or irradiated with neutrons in a VVR-M reactor at 463-543 K [49]. Tensile testing up to 923 K revealed decreases in elongation regardless of the method for He introduction up to 6 appm. Beyond about 6 appm of helium, the uniform elongation reached a plateau of ~20% of the unirradiated elongation value. Another analysis based on early literature tensile results advocated that 2.7 wppm of natural boron or 3 appm of He was sufficient to embrittle Nimonic PE16 [50]. However, no helium measurements or microstructural characterization was conducted to justify this assertion. No studies have been able to separate the effects of helium from solute segregation, so specifying a critical level of helium that would cause embrittlement is not presently possible.

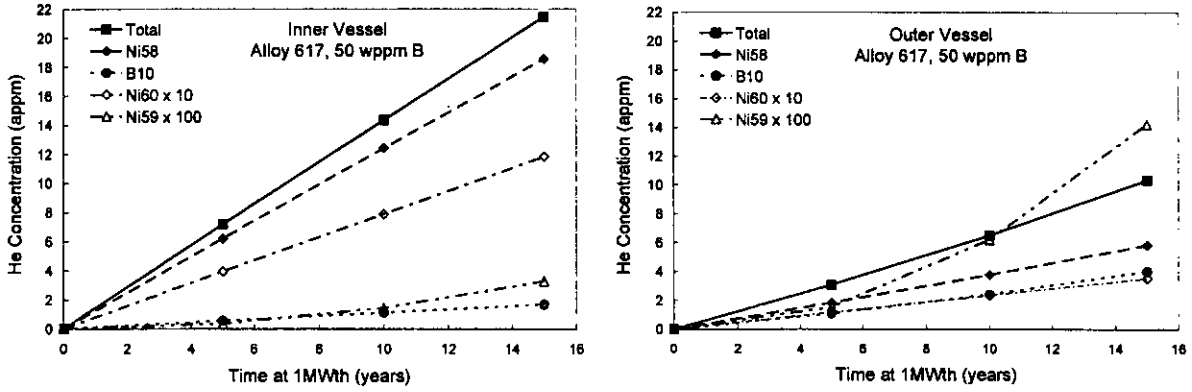

(a) inner vessel for safety rod (thimble) (b) outer vessel.

Figure 10 Calculations showing the amount of helium generated in Alloy 671 containing 50 wppm of natural boron for various isotopes as a function of operational years. (a) inner vessel for safety rod (thimble) and (b) outer vessel. The values shown for ^{59}Ni and ^{60}Ni are multiplied by 100 and 10, respectively.

5. Mitigation of Radiation-Induced Embrittlement

Methods to reduce the effects of irradiation on the high temperature properties of Ni-base alloys have been proposed [24] and investigated by many researchers. The approaches have included removing ^{10}B, reducing the grain size, reducing the grain boundary tensile stress, retaining He within the grains via precipitates (trapping sites), increasing the surface energy to form a void, using grain boundary precipitates to inhibit grain boundary sliding and conducting thermal mechanical treatments prior to irradiation. Examples of studies to explore these remedial methods are briefly reviewed.

Several researchers have reported a beneficial effect of lower boron on post-irradiation ductility. The most significant benefit was reported for Hastelloy X irradiated between 1 to $10x10^{20}$ n/cm^2 (thermal) at unspecified conditions. Figure 11 shows that irradiated Hastelloy X with <0.2 wppm B displayed ~28% total elongation while commercial material, with presumably more boron, exhibited progressively less ductility as the test temperature increased [23]. In another study, only a slight benefit of 1.1 wppm B was observed over 3.8 wppm B when Hastelloy X was

tensile tested at 1173 K after thermal neutron exposure of 2.4×10^{19} n/cm^2 [34], suggesting low sensitivity to helium effects at these conditions. Experiments on PE16 have indicated a beneficial effect of lower boron and thermal treatment on the tensile ductility after irradiation to 20 to 29 dpa (400×10^{20} to 580×10^{20} n/cm^2) in the Dounreay Fast Reactor at 823 K [20]. Reducing the boron content from 82 wppm to 18 wppm resulted in total elongations of over 10% with heat treatment 2 as opposed to several percent with heat treatment 1, Table 10. Heat treatment 1, 1300 K for 0.3 hours + 1023K for 4 hours, produced extensive amounts of intragranular carbides and 10 nm gamma prime. The more ductile heat treatment 2, that included cold rolling and lower temperature treatments, exhibited intragranular TiC, 30nm gamma prime and grain boundaries nearly free of carbides. The mechanism responsible for these results was not reported, however, the lower level of boron in conjunction with boron trapping in the matrix by TiC, may be responsible.

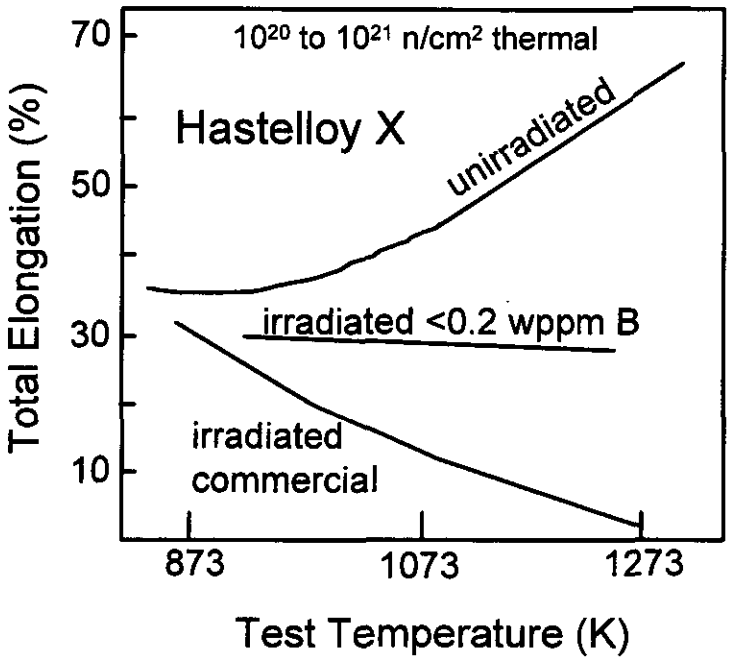

Figure 11 Improvement of post-irradiation tensile ductility of Hastelloy X by lowering the boron content [23].

Table 10 Post-irradiation tensile ductility of Nimonic PE16 as a function of boron and heat treatment . Neutron irradiation of 20 to 29 dpa (4×10^{22} to 5.8×10^{22} n/cm^2) at 823 K [20].

	Percent elongation	
Boron (ppm)	Heat treatment 1 Extensive amounts of intragranular carbides and 10 nm gamma prime	Heat treatment 2 Grain boundaries nearly free of carbides, matrix TiC and 30 nm gamma prime
18	2.3	15.0
37	1.0	6.0
60	0.5	2.2
82		5.8

The premise of boron trapping is to keep helium from reaching the grain boundaries by trapping the inert gas at high energy interfaces of matrix precipitates and to getter boron in these matrix

precipitates. Analysis of Ni-base grain boundaries after solidification and thermal mechanical processing shows that significant boron can exist at Ni-base grain boundaries prior to irradiation. However, collisions with neutrons will displace helium several microns from the location of the originating boron atom, delaying helium embrittlement until the helium atoms diffuse to the grain boundary. The beneficial effects of boron trapping may explain the results shown in Table 10 [20]. Some support for this remedial measure was provided by systematic experiments with Alloy 800 exposed to the mixed spectrum at the Oak Ridge Reactor as a function Ti content [51]. The authors reported that an optimized amount of Ti at 0.1 wt.% exhibited the best post-irradiation creep-rupture ductility and was attributed to the retention of He within the grains at a fine dispersion of Ti-rich precipitates. However, no microscopy was reported to support these claims. In a related study on austenitic stainless steels, a fine matrix distribution of TiC was correlated with improved mechanical properties and was attributed to helium trapping at matrix precipitates [48]. Microstructural characterization showed large bubbles at grain boundaries for material with coarse TiC while almost no grain boundary bubbles were observed for material with fine TiC. Instead, a fine dispersion of voids was observed at matrix TiC precipitates. For Ni-base alloys, oxide dispersion strengthened MA754 was proton irradiated from 723 K to 873 K after helium implantation to assess the effect of incoherent matrix-precipitate interfaces on swelling [52]. Voids were found to nucleate preferably at the oxide-matrix interface, but an expected reduction in swelling was not observed. No mechanical tests were conducted to assess embrittlement.

The effect of pre-irradiation thermal mechanical treatments was investigated for PE16 prior to exposure to 700×10^{20} n/cm^2 (E>0.1 MeV) [53]. Very few or no helium bubbles were observed along grain boundaries for material given a 30% cold work treatment as compared to material annealed after the 30% cold work treatment at 1073K. Microstructural analysis did not reveal matrix TiC precipitates and additional studies were not conducted to further understand these results.

7. Recommendations for Mitigating Radiation-Induced Embrittlement of Prometheus Vessel

A review of the literature and design considerations revealed a concern for the use of a Ni-base alloy pressure vessel for the JIMO mission due to radiation-induced embrittlement. This embrittlement is believed to be a combination of helium and second phase precipitation at grain boundaries, although a full understanding between exposure conditions and material has not been established. Despite this, the primary controlling variables are believed to be the neutron fluence, temperature, stress and alloy condition. Lower fluences are preferred and so are lower stresses at temperatures. These are design considerations that are bounded by the properties of the currently developed commercial materials. However, nickel-base alloys were not designed for neutron exposure at elevated temperatures and the development of nuclear grade materials is warranted. Prior research has shown several promising paths for improving the embrittlement resistance through composition and thermal mechanical treatments. The removal of ^{10}B is evident as a control measure, either by reducing all boron or only ^{10}B. This could be achieved by controlling the boron level during alloy fabrication. The contribution of boron to the mechanical behavior such as the creep strength is not understood, but ^{11}B could be used exclusively to avoid helium transmutation and maintain the properties.

The materials considered for the vessel were primarily Ni-base alloys and the removal of nickel is more of an academic consideration unless cobalt-based alloys are considered. In these alloys, the nickel content would be reduced by approximately a factor of two to three for commercially available cobalt-based alloys, such as Haynes 188 (39Co-22Ni-22Cr-14W).

Cobalt-59 has 1/50 of the n,α reaction rate as ^{58}Ni and would produce 1/50 as much helium by the threshold reaction

$$^{59}Co + n_f \rightarrow {}^{56}Mn + {}^{4}He. \quad (5)$$

Solute segregation can be reduced by lowering the levels of Al, Nb, Ti and Si as well as keeping metalloids very low. Examples of radiation resistant Ni-base alloy compositions are shown in Table 2. The nuclear grade (NG) versions stay within the current composition specification while reducing elements believed to be responsible for helium embrittlement (boron) and intermetallic formation resulting from solute segregation (Al, Si, Ti). The low (L) grade versions go beyond the current specifications. Screening experiments are recommended to determine structure to property relationships with comparisons to commercially available materials. One such study was proposed, but was abandoned when the program was restructured (see Attachment).

8. Conclusions

Radiation damage was a major concern for Ni-base structural materials considered for the JIMO mission. A literature review and helium transmutation calculations revealed the conclusions:

1. Ni-base alloys are significantly embrittled after neutron exposure at elevated temperatures. This embrittlement has been attributed to a combination of helium and second phase precipitation at grain boundaries.
2. Experimental studies are required to assess radiation-induced embrittlement under prototypical conditions.
3. Radiation-induced swelling and creep would not be expected to exceed design allowables of 1% each.
4. It is strongly recommended that nuclear grade Ni-base and cobalt-based alloys be pursued as a method to mitigate radiation-induced embrittlement by reducing helium generation and solute segregation.
5. Alternative designs to the inner safety rod pressure vessel (thimble) need to be seriously pursued as the current understanding indicates that a Ni-base alloy thimble may be significantly embrittled by radiation.

References

1. MDO-723-0010, Summary of Structural Materials Considered for the Prometheus Space Nuclear Power Plant (SNPP), January 2006.
2. J.L. Laidler, J.J. Holmes and J.W. Bennett, "U.S. Programs on Reference and Advanced Cladding/Duct Materials", International Conference: Radiation Effects in Breeder Reactor Structural Materials, American Institute of Mining, Metallurgical and Petroleum Engineers (1977) pages 41-52.
3. R.W. Powell, "Superalloys in Fast Breeder Reactor", HEDL-SA-811, Jan. 1976.
4. J.L. Straalsund, R.W. Powell and B.A. Chin, "An Overview of Neutron Irradiation Effects in LMFBR Materials", J. Nuclear Materials, vol. 108 & 109 (1982) 299-305.
5. J.F. Bates and R.W. Powell, "Irradiation-Induced Swelling in Commercial Alloys", Journal of Nuclear Materials, 102 (1981) pages 200-213.
6. R. Bajaj, R.P. Shogan, C. DeFlitch, R.L. Fish, M.M. Paxton and M.L. Bleiberg, "Tensile Properties of Irradiated Nimonic PE16", 10th International Symposium on Effect of Radiation on Material, ASTM STP 725 (1981) pages 326-351.
7. R.M. Boothby, "The Microstructure of Fast Neutron Irradiated Nimonic PE16", Journal of Nuclear Materials, vol. 230 (1996) pages 148-157.

8. A.F. Rowcliffe, "Irradiation Performance of Nickel-Base Superalloys", Critical Assessment of Structural Materials for Space Nuclear Applications, S. Zinkle et. al., ORNL/LTR/NR-JIMO/04-08, September 2005.
9. K.F. Allbeson, C. Brown and J. Gillespie, "PE16 and the Role of PFR in its Validation as an Advanced FBR Fuel Pin Cladding Material", The Nuclear Engineer, vol. 31, no. 1 (1990) pages 87-89.
10. C. Brown et al., in Proc. Int. Conf. on Fast Reactor and Related Fuel Cycles Kyoto (1991) vol. 1 pages 7.5.1 to 7.5.10.
11. M. Naganuma et. Al., High Burn-up Irradiation Performance of Annular Fuel Pins Irradiated in PFR, in Proc. IAEA Conf on MOX Fuel Cycles Technologies for Medium and Long-Term Deployment, IAEA (2000) page 556.
12. Haynes Alloy 188, Haynes High-Temperature Alloys (1991).
13. K. Natesan, A. Purohit, S.W. Tam, "Materials Behavior in HTGR Environments", NUREG/CR-6824, ANL-02/37, Argonne National Laboratory, July 2003, pages 19-24.
14. MDO-723-0044 / B-MT(SRME)-52, "JOYO-1 Irradiation Test Campaign Technical Close-Out, For Information, February 2006.
15. J.I. Bramman, C. Brown, J.S. Watkin, C. Cawthorne, E.J. Fulton, P.J. Barton and E.A. Little, "Void Swelling and Microstructural Changes in Fuel Pin Cladding and Unstressed Specimens Irradiated in DFR", International Conference: Radiation Effects in Breeder Reactor Structural Materials, The Metallurgical Society of AIME (1977) pages 479-507.
16. J.S. Watkins, J.H. Gittus and J. Standring, "The Influence of Alloy Constitution on the Swelling of Austenitic Stainless Steels and Nickel Based Alloys", International Conference: Radiation Effects in Breeder Reactor Structural Materials, The Metallurgical Society of AIME (1977) pages 467-477.
17. W.K. Appleby, D.W. Sandusky and U.E. Wolff, "Swelling Resistance of a High Nickel Alloy", Journal of Nuclear Materials, vol. 43 (1972) pages 213-218.
18. M.M. Paxton, B.A. Chin, E.R. Gilbert and R.E. Nygren, "Comparison of the In-Reactor Creep of Selected Ferritic, Solid Solution Strengthened, and Precipitation Hardened Commercial Alloys", Journal of Nuclear Materials, vol. 80 (1979) pages 144-151.
19. A.J. McSherry and M. Patel, "Results from the First Interim Examination of the Advanced Alloy Creep In-Bending Test", National Cladding/Duct Materials Development Program Quarterly Technical Progress Letter, TC-160-21, Hanford Engineering Development Laboratory (1979) pages 3-8.
20. J. Barnaby, P.J. Barton, R.M. Boothby, A.S. Fraser and G.F. Slattery, "The Post-Irradiation Mechanical Properties of AISI Type 316 Steel and Nimonic PE16 Alloy", International Conference: Radiation Effects in Breeder Reactor Structural Materials, The Metallurgical Society of AIME (1977) pages 159-175.
21. K.E. Moore, R.G. Brengle, T.G. Parker, "Hastelloy X Cladding Materials Evaluation", SNAP Reactor, SNAP Program C-92b, AI-AEC-13083 (1973).
22. K.S. Lee, "Creep Rupture Properties of Hastelloy-X and Incoloy-800H in a Simulated HTGR Helium Environment Containing High Levels of Moisture," Nuclear Technology, vol. 66 (1984) page 241.
23. J.R. Lindgren, "Irradiation Effects on High-Temperature Gas-Cooled Reactor Structural Materials", Nuclear Technology, vol. 66 (1984) pages 607-618.
24. D.R. Harries, "Neutron Irradiation Embrittlement of Austenitic Stainless Steels and Nickel Base Alloys", Journal of the British Nuclear Energy Society, vol. 5 (1966) pages 74-87.
25. L.K. Mansur, E.H. Lee, P.J. Maziasz and A.P. Rowcliffe, "Control of Helium Effects in Irradiated Materials Based on Theory and Experiment", vol. 141-143 (1986) pages 633-646.
26. H. Schroeder, "High Temperature Embrittlement of Metals by Helium", Radiation Effects, vol. 78 (1983) pages 297-314.

27. R.M. Boothby, "Lithium and Helium Embrittlement of Nimonic PE16", Journal of Nuclear Materials, vol. 186 (1992) pages 209-211.
28. G.A. Young, R. Najafabadi, W. Strohmayer, D.G. Baldrey and W.L. Hamm, "An Atomistic Modeling Study of Alloying Element, Impurity Element, and Transmutation Products on the Cohesion of a Nickel S5 {001} Twist Grain Boundary", 11th International Conference on the Environmental Degradation of Materials in Nuclear Systems, Stevenson, WA (2003) pages 758-769.
29. R.W. Smith, W.T. Geng, C.B. Geller, R. Wu and A.J. Freeman, "The Effect of Li, He and Ca on Grain Boundary Cohesive Strength in NI", Scripta Materialia, V43 (2000) pages 957-961.
30. H.J. Busboom and P.W. Mathay, "Fast Neutron Damage Studies in High Nickel Alloys", General Electric Atomic Power report, GEAP-4985, AEC Research and Development Report, August 1966.
31. F.A. Garner, B.M. Oliver and L.R. Greenwood, "The dependence of Helium Generation Rate on Nickel Content of Fe-Cr-Ni Alloys Irradiated to High dpa Levels in EBR-II", Journal of Nuclear Materials, vol. 258-263 (1998) pages 1740-1744.
32. L.R. Greenwood, "A New Calculation of Thermal Neutron Damage and Helium Production in Nickel", Journal of Nuclear Materials, vol. 115 (1983) pages 137-142.
33. L.R. Greenwood, F.A. Garner, B.M. Oliver, M.L. Grossbeck and W.G. Wolfer, "Surprisingly Large Generation and Retention of Helium and Hydrogen in Pure Nickel Irradiated at High Temperatures and High Neutron Exposures", Journal of ASTM International, Paper ID JAI11365, vol. 1, no. 4 (2004) pages 529-539.
34. K. Watanabe, Y. Ogawa, M. Kikuchi and T. Kondo, "Ductility Loss of Neutron-Irradiated Hastelloy-X at Elevated Temperatures, JAERI Research Report JAERI-M 8807 (April 1980).
35. T. Kondo, "Development and Testing of Alloys for Primary Circuit Structures of a VHTR", Specialists' Meeting on High Temperature Metallic Materials for Application in Gas-Cooled Reactors, Vienna, Austria, May 4-6, 1981. IAEA, International Working Group on Gas-Cooled Reactors, IWGGCR-4.
36. R.M. Boothby, "Modelling Grain Boundary Cavity Growth in Irradiated Nimonic PE16", Journal of Nuclear Materials, vol. 171 (1990) pages 215-222.
37. D.R. Harries, "Review Neutron Irradiation-Induced Embrittlement in Type 316 and Other Austenitic Steels and Alloys", Journal of Nuclear Materials, vol. 82 (1979) pages 2-21.
38. T.R. Allen, J.T. Busby, G.S. Was and E.A. Kenik, "On the Mechanism of Radiation-Induced Segregation in Austenitic Fe-Cr-Ni Alloys", Journal of Nuclear Materials, vol. 255 (1998) pages 44-58.
39. R.A. Mulford, C.J. McMahon, D.P. Pope and H.C. Feng, Metallurgical Transactions A, vol. 7A (1976) pages 1183-1195.
40. P.S. Sklad, R.E. Clausing and E.E. Bloom, "Effect of Neutron Irradiation on Microstructure and Mechanical Properties of Nimonic PE-16", in F.R. Shober (ed.) Irradiation Effects on the Microstructure and Properties of Metals". ASTM STP 611, American Society for Testing and Materials, Philadelphia (1976) pages 139-155.
41. W.J.S. Yang, "Grain Boundary Segregation in Solution-Treated Nimonic PE16 During Neutron Irradiation", Journal of Nuclear Materials, vol. 108 & 109 (1982) 339-346.
42. W.J. S. Yang, L.E. Thomas, D.S. Gelles and J.L. Straalsund, "The Role of Solute Segregation in Postirradiation Ductility Loss", National Cladding/Duct Materials Development Program Quarterly Technical Progress Letter, TC-160-21, Hanford Engineering Development Laboratory (1979) pages 262-282.
43. W.J. S. Yang, "Microstructures of Solution-Treated, Unirradiated Nimonic PE16 and Inconel 706 Duct Materials in the Ductility Trough", National Cladding/Duct Materials Development Program Quarterly Technical Progress Letter, TC-160-20, Hanford Engineering

Development Laboratory (1979) pages 187-196.
44. R. Bajaj, C. DeFlitch, R.P. Shogan and M.L. Bleiberg, "Special Tensile Tests on Advanced Alloys", National Cladding/Duct Materials Development Program Quarterly Technical Progress Letter, TC-160-20, Hanford Engineering Development Laboratory (1979) pages 261-271.
45. R. Bajaj, R.P. Shogan and D. DeFlitch, "Special Tensile Tests on Advanced Alloys", National Cladding/Duct Materials Development Program Quarterly Technical Progress Letter, TC-160-18, Hanford Engineering Development Laboratory (1978) pages 229-240.
46. B. Bohm and K.-D. Gloss, "Effects of Strain Rate on High Temperature Mechanical Properties of Irradiated Incoloy 800 and Hastelloy X", Radiation Effects in Breeder Reactor Structured Materials, eds. M.L. Bleiberg & J.W. Bennett, TMS (1977) pages 347-356.
47. Sutton, T.M., Brown, F.B., Bischoff, F.G., MacMillan, D.B., Ellis C.L., Ward, J.T., Ballinger, C.T., Kelly, D.J., Schindler, L., "The Physical Models and Statistical Procedures Used in the RACER Monte Carlo Code," KAPL-4840, UC-505, DOE/TIC-4500-R75, Knolls Atomic Power Laboratory, July 1999. TIS-866-3120, March 22, 2000.
48. W. Kesternich, "A Possible Solution of the Problem of Helium Embrittlement", Journal of Nuclear Materials, vol. 127 (1985) pages 153-160.
49. V.F. Vinokurov, I.V. Gorynin, G.T. Zhdan, Sh.Sh. Ibragimov, O.A. Kozhevnikov, V.F. Reutov, S.A. Fabritsiev and V.D. Yaroshevich, "Influence of Helium Upon the Structure, the Strength, and the Plasticity of Alloys with High Nickel Content", (1987) pages 194-203.
50. R.S. Barnes, "Embrittlement of Stainless Steels and Nickel-Based Alloys at High Temperature Induced by Neutron Radiation", Nature vol. 206 (1965) pages 1307-1310.
51. D.G. Harman, "Post Irradiation Tensile and Creep-Rupture Properties of Several Experimental Heats of Incoloy 800 at 700 and 760C", Oak Ridge National Lab, ORNL-TM-2305 (December 1968).
52. H. Shiraishi and A. Hasegawa, "Helium Effects in Iron- and Nickel-Base Developmental Alloys", Journal of Nuclear Materials, vol. 155-157 (1988) pages 1049-1053.
53. A.L. Chang and M.L. Bleiberg, "Comparison of Microstructures in Neutron Irradiated Nimonic PE16 of Different Thermal Mechanical Treatments", National Cladding/Duct Materials Development Program Quarterly Technical Progress Letter, TC-160-27, Hanford Engineering Development Laboratory (1980) pages 199-205.
54. D.J. Mazey, W. Hanks, D.E.J. Bolster and B.C. Sowden, "Cavitation and Swelling in Nimonic PE16 Alloy Under Ion Irradiation to Simulate Fusion-Reactor Irradiation Conditions", Nuclear Energy, vol. 28, no. 2 (1989) pages 97-110.
55. Nimonic alloy PE16, Special Metals Publication Number SMC0102 (2004) page 19.
56. P.C.L. Pfeil and D.R. Harries, "Effects of Irradiation in Austenitic Steels and Other High-Temperature Alloys", Flow and Fracture of Metals and Alloys in Nuclear Environments, ASTM Special Technical Publication no. 380, ASTM (1964) pages 202-221.
57. F.-H. Huang and R.L. Fish, "Ring Ductility of Irradiated Inconel 706 and Nimonic PE16", Effects of Radiation on Materials: Twelfth International Symposium, ASTM STP 870, F.A. Garner and J.S. Perrin, eds., American Society for Testing and Materials, Philadelphia (1985) pages 720-731.
58. T.T. Claudson and H.J. Pessl, "Irradiation Effects on High-Temperature Reactor Structural Metals", Flow and Fracture of Metals and Alloys in Nuclear Environments, ASTM Special Technical Publication 380, ASTM (1964) pages 156-170.

Attachment 1 to
MDO-723-0043

Assessing the Effects of Radiation Damage on Ni-base Alloys for the Prometheus Space Reactor System

Evaluating the Effects of Composition and Microstructure Evolution on the Radiation-Induced Embrittlement of Candidate Prometheus Pressure Vessel Materials at HFIR

Author:
Tom Angeliu

Introduction

Nickel-based alloys are promising materials for structural applications in high temperature nuclear reactors. These materials have a well-developed commercial fabrication infrastructure, and their long-term thermal creep behavior is reasonably well known. However, the largest uncertainty is grain boundary embrittlement due to radiation-induced solute segregation and/or the accumulation of helium produced by transmutation. Studies have shown that these processes become more pronounced with increasing temperature and are dependent on the alloy composition. Systematic studies have not been conducted to correlate helium concentration and solute segregation to the mechanical properties.

Previous studies on the radiation-induced embrittlement of Ni-base alloys at elevated temperatures are limited. Helium embrittlement results when Ni and ^{10}B transmutate to helium, which migrates to forms grain boundary voids. The $^{10}B(n, \alpha)$ reaction has a very high thermal neutron cross section and a significant epithermal cross section. Although the thermal neutron flux would be very low in a fast reactor spectrum, the epithermal neutron flux may be sufficiently large to readily transmute all of the ^{10}B, which is 20% of the total natural boron. Some helium generation will also occur from the two-sequential step $^{58}Ni(n,\gamma)^{59}Ni(n,\alpha)$ nuclear reaction that has a nonlinear dependence on neutron fluence. Mitigation of this phenomena was demonstrated with two ultra-low boron-containing commercial Ni-base alloys, PE16 and Hastelloy X (<0.02 wppm B), that exhibited improved tensile ductility as compared to commercial materials containing 50 to 100 wppm B after neutron exposure [A1, A2]. The segregation of precipitate forming elements to grain boundaries has also been implicated with embrittlement. Elements such as Al, Ti and Nb segregate to form continuous networks of second phases at grain boundaries, promoting a severe loss in ductility [A3]. Silicon has also been implicated in grain boundary embrittlement through the formation of silicides.

The overall purpose of these studies is to identify a Ni-base alloy that is resistant to radiation-induced embrittlement for core components, such as the Prometheus reactor pressure vessel. This would have been achieved by understanding the effects of neutron irradiation on the mechanical behavior and correlating these results to the composition and microstructural evolution. The mixed thermal and fast neutron spectrum at the High Flux Isotope Reactor (HFIR) at Oak Ridge National Lab (ORNL) is more representative of a fast spectrum than proton, electron or ion irradiation. The disadvantage of HFIR is that the thermal spectrum may transmute a disproportional amount of Ni to Fe and He and promote more embrittlement than in a fast spectrum. The fast reactor at JOYO is a more representative test facility, but the test space is limited and the time and effort to conduct experiments at JOYO are considerably more.

There are many variables to consider when planning for this study, including materials, temperatures, fluences and test specimens. The proposed baseline test matrix consisted of swelling, tensile testing and microstructure characterization of 9 materials, including both commercial and controlled purity alloys. Five alloys are commercial materials and four are controlled purity variants of Ni-base materials Alloy 617 and Haynes 230, Table A1. Three of the commercial alloys would have been exposed in JOYO-1. The remaining commercial alloys were promising materials that were not included in JOYO-1 due to space constraints. Each of the proposed materials is described briefly below.

Table A1 Proposed Compositions for Radiation-Induced Embrittlement Studies (wt. %)

Alloy	Ni	Cr	Fe	W	Mo	Co	Mn	Si	Al	Ti	C	B	other
617*	Bal.	20-24	<3	-	8-10	10-15	<1	<1	0.8-1.5	<0.6	0.05-0.15	<0.006	S <0.015
617NG	Bal.	22	-	-	9	12.5	0.3	0.25	0.8	0.3	0.08	<20ppm	
617L	Bal.	22	-	-	9	12.5	0.3	-	-	-	0.08	<20ppm	
230**	Bal.	20-24	<3	13-15	1-3	<5	0.3-1.0	0.25-0.75	0.2-0.5	-	0.05-0.15	<150ppm	P <0.030 S <0.01 La0.005-0.050
230NG	Bal.	22	-	14	2	0.5	0.3	0.25	0.2	-	0.10	<20ppm	0.02La
230L	Bal.	22	-	14	2	0.5	0.3	-	-	-	0.10	<20ppm	0.02La
HastX	Bal.	22	18	0.6	9	1.5	<1	<1	-	-	0.15	<80ppm	
HastXNG	Bal.	22	18	0.6	9	1.5	<1	-	-	-	0.15	<20ppm	
PE16*	42-45	15.5-17.5	Bal.	-	2.8-3.8	<2	<0.2	<0.5	1.1-1.3	1.1-1.3	0.04-0.08	<50ppm	0.02-0.04Zr
PE16NG	43	16	Bal.	-	3.2	<2	<0.2	-	1.1	1.1	0.06	<20ppm	0.03Zr
HS188#	20-24	21-23	<3	13-15	-	Bal.	<1.25	0.2-0.5	-	-	0.05-0.15	<150ppm	0.02-0.12La
HS188NG	22	22	-	14	-	41	<1.25	-	-	-	0.10	<20ppm	0.07La
MA754*	Bal.	20	1	-	-	-	-	-	0.3	0.5	0.05	-	$0.6Y_2O_3$
PM2000*	-	19	Bal.	-	-	-	-	-	5.5	0.5	-	-	$0.5Y_2O_3$

* From Special Metals Bulletin ** From ASME code case # From Haynes Bulletin
Tramp elements such as S, P, N, O shall be as low as reasonably possible.

Commercial alloys

Nimonic PE16: This precipitation hardened Ni-base alloy has a complex microstructure containing gamma prime (γ') and carbide precipitates. The effects of irradiation on Ni-base alloys have been studied the most for this material. PE16 was successfully used as fast reactor fuel cladding, achieving exposures up to 1000K in excess of $1400x10^{20}$ n/cm^2 with only four failures in over 16,500 clad pins [A4]. However, PE16 exhibits a significant decrease in tensile ductility with irradiation, attributed to a combination of helium embrittlement and the precipitation of second phases at grain boundaries [A5, A6] or differential strengthening of the matrix relative to the grain boundaries [A7].

Alloy 617: This is a solid solution strengthened Ni-base alloy that contains carbide and gamma prime precipitates, although the gamma prime contributes little to the strength. Alloy 617 is a promising alloy for Generation IV high temperature gas reactor heat exchanger applications and has an extensive database for unirradiated mechanical properties. No radiation studies have been conducted on this material.

Alloy 230: This material is solid solution strengthened Ni-base alloy with carbide precipitates. It has also been considered for Generation IV applications along with Alloy 617. No radiation studies have been conducted on this material.

Hastelloy X: This is a solid solution strengthened material that was investigated on a limited basis in previous reactor programs. This material exhibited a significant decrease in tensile ductility upon irradiation, attributed to helium embrittlement. Alloys 617 and 230 have slightly improved mechanical properties over Hastelloy X.

Alloy 188: This cobalt-based material is solid solution strengthened and has mechanical properties comparable to Alloys 617 and 230. Cobalt materials have not been considered for many reactor applications because of the activation of ^{60}Co. Co-based alloys are expected to

be more resistant to He embrittlement (lower levels of Ni) and solute segregation (no Al, Ti or Nb) compared to Ni-base alloys. Alloy 188 contains only 22 wt.% Ni as opposed to 54 to 57 wt.% for Alloys 617 and 230, resulting in ~2.5 times less helium production.

MA754: This material is a Ni-base oxide dispersion strengthened material (ODS) that has promising thermal creep behavior, but very poor weldability. No radiation studies have been conducted on this material, but it contains the potentially embrittling elements of Al and Ti.

PM2000: This material is a ferritic ODS material that has promising thermal creep behavior, but very poor weldability. Previous HFIR exposure on a closely related alloy, MA956, was inconclusive because of experimental difficulties [A8]. Many of the tensile specimens bonded together during the irradiation, hence sparse data was generated. However, the structure exhibited relatively little damage.

Controlled Chemistry Alloys

Alloys 617 and 230 were selected to improve their resistance to radiation-induced embrittlement by slightly modifying their chemical compositions. These materials were selected because they have the most promise for improved behavior by limiting several elements believed to promote radiation-induced embrittlement, which are Al, Ti, Nb, B and Si. A nuclear grade version of each alloy would lower these elements to the minimum allowable of the commercial specification limit. A controlled purity version of each alloy would reduce these elements as low as reasonably possible to determine the maximum amount of embrittlement resistance that could be expected from this approach.

A design of experiments analysis was applied to the Ni-base compositions being proposed and is shown in Table A2. The primary mechanical property of interest is ductility. The embrittlement mechanisms are He embrittlement (from B and Ni transmutation) and grain boundary solute segregation (Al, Ti and Si) leading to the formation of intermetallic phases. It is assumed that all materials would contain a low level of damaging segregating impurities such as S, P, etc. From this analysis, improvements in the % elongation are anticipated by minimizing the effects of helium and grain boundary phases.

Table A2 Design of Experiment Analysis for the Proposed HFIR Studies

							After Irradiation			
	Alloy	Fe, Cu, etc.	Si	Al	Ti	B	He (appm)	GB phases	% elong.	comments
1	Commercial A617	+	+	+	+	+	+	+	low	
2	617NG	-	+	0	+	-	-	+?	?	Within material spec.
3	617L	-	-	-	-	-	-	-	high	Al, Ti, Si below spec.
4	Commercial 230	+	+	+	-	+	+	+	low	
5	230NG	-	+	0	-	-	-	+?	?	Within material spec.
6	230L	-	-	-	-	-	-	-	high	Al, Ti, Si below spec
7	Commercial HastX	+	+	-	-	+	+	-?	low	
8	HastXNG	+	-	-	-	-	-	-	high	Within material spec.
9	Commercial PE16	+	+	+	+	+	+	+	low	
10	PE16NG	+	-	+	+	-	-	+	high?	Within material spec.
11	HS188	-	-	-	-	+	+	-?	low	Cobalt based
12	HS188NG	-	-	-	-	-	-	-?	high	Within material spec.

+ means high, - means low, 0 is an intermediate level, ? is unknown

HFIR Irradiation Conditions

All 9 alloys of the baseline matrix would be irradiated at one fluence of $20x10^{20}$ n/cm^2 (1 dpa) at two irradiation temperatures of 850 K and 1050 K. It is believed that most of the ^{10}B will transmutate to He at this fluence [A9] while solute segregation effects may saturate at higher fluences, such as $200x10^{20}$ n/cm^2 (10 dpa) [A3]. It is possible that greater fluences would be required to understand the limits of the controlled purity materials as the application may involve fluences up to $80x10^{20}$ n/cm^2 for the vessel and $160x10^{20}$ n/cm^2 for the thimble. Helium calculations would determine the amount of transmutant helium to expect in HFIR and adjustments to the dosage would be made to ensure that the helium was representative of that produced in a fast spectrum. The temperatures proposed are based on the JOYO-1 test matrix, where the majority of the data would have been generated at 850 K and 1050 K. Table 3 lists all of the proposed alloys and their compositions. Six of the ten alloys proposed in this HFIR study would have been exposed in JOYO-1 if the controlled purity heats were fabricated in time.

Table A3 Comparing the JOYO-1 Test Plan With The Proposed HFIR Experimental Options

	Alloy	JOYO-1	HFIR-A	HFIR-B	HFIR-C
1	Commercial 617	X	X	X	X
2	617NG	a	X	X	XX
3	617L	a	X	X	XX
4	Commercial 230	X	X	X	X
5	230NG	a	X	X	XX
6	230L	a	X	X	XX
7	Commercial PE16	X	X	X	X
8	PE16NG			X	XX
9	Commercial HastX		X	X	X
10	HastX NG			X	XX
11	HS 188		X	X	X
12	HS 188 NG			X	XX
13	MA754			X	X
14	PM2000			X	X
	Test conditions	20 to $75x10^{20}$ n/cm^2 850, 950, 1050 K	$20x10^{20}$ n/cm^2 850, 1050 K	$20x10^{20}$ n/cm^2 850, 1050 K	20 & $80x10^{20}$ n/cm^2 850, 1050 K
	Estimated Completion	(~24 mon.)	(14 mon.)	(14 mon.)	?
	Cost estimate		$819K	$1100K	$1700K

NG denotes low level of embrittling elements, but within the chemistry specification
L denotes low level of embritling elements, below the chemistry specification
a – If material can be fabricated in time for insertion
XX – exposed to $80x10^{20}$ n/cm^2

In this study, understanding the radiation-induced embrittlement relies on tensile data and microstructural examinations to develop structure-property relationships. Four tensile specimens of each alloy would be exposed at 850 K and 1050 K for a total of 8 specimens per alloy. After irradiation, two specimens would be tested at the irradiation temperature and one at room temperature, with one specimen held in reserve. The tensile testing would report the yield and tensile strengths along with the percent elongation to failure. Up to 10 fracture surfaces would be examined using a hot cell scanning electron microscope (SEM) to determine the

amount of ductile, transgranular and intergranular fracture morphology and reduction in area. Up to 10 examinations would be conducted using a field emission (high resolution) transmission electron microscope FEG-TEM. At least 2 TEM foils would be examined from each selected condition, with the samples coming from the shoulders of the tensile specimens. The FEG-TEM analysis of the microstructure would include images and observations of the matrix and grain boundary structure, the quantification of voids and precipitates, and the chemical analysis of several grain boundaries, including 2 composition profiles across a grain boundary as well as several spot checks on grain boundaries and / or grain boundary / precipitate interface. A summary of the expected results are shown in Table A4 and schematically in Figure A1.

Table A4 Summary of Anticipated Results

Alloy	Temp, K	Fluence, n/cm^2	Density	σ_{ys}, MPa	σ_{UTS}, MPa	% elong.	Fracture toughness	SEM	He, appm	GB struc	GB comp	Matrix struc
A617	298	$20x10^{20}$										
	850	$20x10^{20}$										
	1050	$20x10^{20}$										
617NG	298	$20x10^{20}$										
	850	$20x10^{20}$										
	1050	$20x10^{20}$										
617L	298	$20x10^{20}$										
	850	$20x10^{20}$										
	1050	$20x10^{20}$										
Etc...												

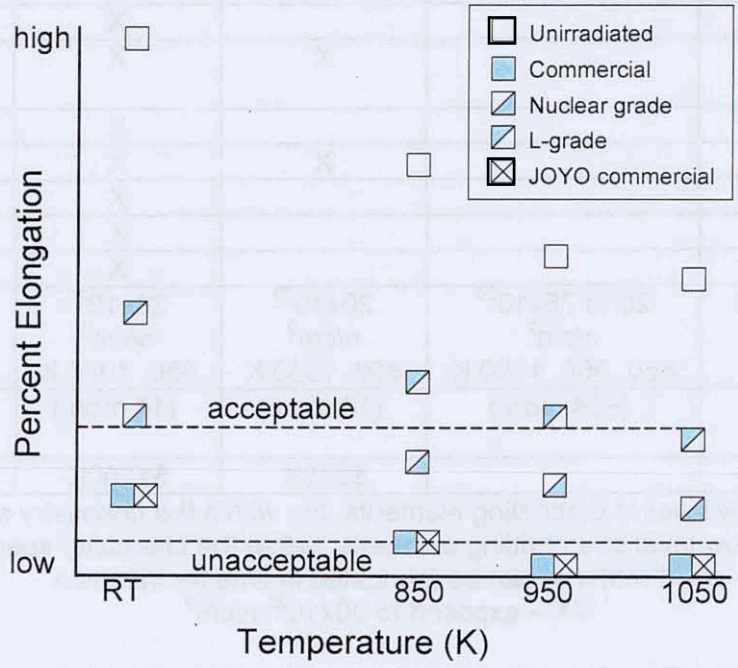

Figure A1 Schematic showing a summary of the anticipated results.

Density measurements would examine the swelling behavior of all materials. Passive thermal monitors would determine the temperature at the end of the exposure.

Comparison of HFIR and JOYO

The replication of test conditions in HFIR and JOYO-1 [A10] would allow for comparisons between mixed and fast spectrums. This would be useful for determining whether future studies can produce reasonable results at the more accessible HFIR facility or if future studies need to be conducted only at more expensive fast spectrum facilities. Exposure in JOYO is the most representative neutron environment as it is a fast reactor. There was space in JOYO-1 to conduct a very limited evaluation of several controlled purity alloys by removing redundant commercial Ni-base alloy tensile specimens. HFIR testing was necessary because the test space in JOYO-1 was limited and not all of the materials of interest could be evaluated within the schedule. HFIR was attractive because it was readily available and there was an established program already with ORNL on HFIR testing. Table A3 summarizes the comparisons available after both HFIR and JOYO-1 are complete.

Experimental Options

The test conditions outlined above are for a baseline study designated as HFIR-A in Table A3. Expansion of this matrix should consider the following options.

Materials. The test matrix may be expanded to include nuclear grade versions of other materials such as PE16, Hastelloy X and HS188. These materials would contain ultra-low levels of boron compared to the commercial materials to complement the study of Alloys 617 and 230. MA754 is an ODS Ni-base alloy that may have unique resistance to radiation-induced embrittlement. The high energy, incoherent boundaries provided by the oxide-matrix interface may attract helium and detrimental elements rather than grain boundaries. These material options are summarized as HFIR-B in Table A3.

Fluences. The nuclear grade and L-grade materials may require a higher dose before embrittlement effects are observed and saturated. Four ($80x10^{20}$ n/cm^2) or more HFIR cycles may be necessary to determine the limitations of these materials as well as to be more representative of the final vessel fluence. This option is summarized as HFIR-C in Table A3.

Fracture Toughness. Crack propagation is an important design consideration that is evaluated through the fracture toughness behavior. Tensile ductility is related to fracture toughness, but tensile data need to be correlated to the fracture toughness. It is proposed that some fracture toughness experiments be included in the baseline study to determine the feasibility of this approach for future studies.

Creep Rupture Ductility. It is important to learn the effect of irradiation on the creep rupture ductility. This may be assessed by post-irradiation testing of creep specimens. It is proposed that some post-irradiation creep experiments be considered to determine the feasibility of this approach.

The cost of each additional material exposed at one fluence and two temperatures is ~$50K. This is based on the fixed costs for the baseline study estimated to be ~$363K of the total ~$819K. Additional materials would not alter the schedule significantly, but additional fluences would push back the schedule according to the HFIR schedule. The estimated cost for fracture toughness and creep testing needs to be determined.

Recommendations

It is recommended that the baseline study be implemented, HFIR-A. HFIR options B, C and derivatives of these can be pursued in the future based on the results of the initial study or immediately if the risk to the program is perceived to be very high and the funding is available.

Cost Estimate for the Baseline Study of 9 Compositions $819K

Fixed costs:	$363K	
Program Management	150K	
Design and Safety Calcs	90K	
Evaluation Setups & Sorting	84K	
Transport & Disposal	39K	
Variable costs:	$456K	each composition is about $50K
Capsules	28K	
Tensile (hot cell)	220K	
Fracture toughness		
Irradiation	60K	
Passive thermometry	30K	
Swelling (hot cell)	20K	
SEM (hot cell)	32K	
TEM	52K	
Transport & Disposal	64K	

References

A1. A.F. Rowcliffe, "Irradiation Performance of Nickel-Base Superalloys", Critical Assessment of Structural Materials for Space Nuclear Applications, S. Zinkle et. al., ORNL/LTR/NR-JIMO/04-08, September 2005.

A2. J. Barnaby, P.J. Barton, R.M. Boothby, A.S. Fraser and G.F. Slattery, "The Post-Irradiation Mechanical Properties of AISI Type 316 Steel and Nimonic PE16 Alloy", International Conference: Radiation Effects in Breeder Reactor Structural Materials, The Metallurgical Society of AIME (1977) pages 159-175.

A3. J.R. Lindgren, "Irradiation Effects on High-Temperature Gas-Cooled Reactor Structural Materials", Nuclear Technology, vol. 66 (1984) pages 607-618.

A4. K.F. Allbeson, C. Brown and J. Gillespie, "PE16 and the Role of PFR in its Validation as an Advanced FBR Fuel Pin Cladding Material", The Nuclear Engineer, vol. 31, no. 3 (1990) pages 87-89.

A5. R.M. Boothby, "The Microstructure of Fast Neutron Irradiated Nimonic PE16", Journal of Nuclear Materials, vol. 230 (1996) pages 148-157.

A6. W.J.S. Yang, "Grain Boundary Segregation in Solution-Treated Nimonic PE16 During Neutron Irradiation", Journal of Nuclear Materials, vol. 108 & 109 (1982) 339-346.

A7. R. Bajaj, R.P. Shogan, C. DeFlitch, R.L. Fish, M.M. Paxton and M.L. Bleiberg, "Tensile Properties of Irradiated Nimonic PE16", 10th International Symposium on Effect of Radiation on Material, ASTM STP 725 (1981) pages 326-351.

A8. D.J. Perry, TP-382 Phase 1 Post-Irradiation Examination (PIE) Results for Hastelloy N and MA956 (U), Materials Development Operation, Structural Materials Engineering Technical Data Memorandum No. 525 (TDM-525), March 29, 2002.

A9. T. Kondo, "Development and Testing of Alloys for Primary Circuit Structures of a VHTR", Specialists' Meeting on High Temperature Metallic Materials for Application in Gas-Cooled Reactors, Vienna, Austria, May 4-6, 1981. IAEA, International Working Group on Gas-Cooled Reactors, IWGGCR-4.

A10. MDO-723-0011 & B-MT(SRME)-53, Refractory Metal Irradiation Testing at Oak Ridge National Lab (U), 2006.

Distribution to
MDO-723-0043

CONCURRENCE/DESIGN CHECK FORM FOR DOCUMENT NO. MDO-723-0043 **Date:** Jan. 18, 2006

DOCUMENT TITLE: **Assessing the Effects of Radiation Damage on Ni-base Alloys for the Prometheus Space Reactor System (for information only)**

REFERENCES _____ ENCLOSURES: _____

1. ADSARS: PERMANENT RECORD: Yes X No ___ Repository MFLIB Corporate Author: KAPL NR PROGRAM ___

Key Words:	Ni-base alloys	Radiation Embrittlement	Helium Embrittlement	Transmutation	Prometheus				
Need to Know Categories	GEN								
Available Sites:									
Design File Location(s)									

2. DESIGN CHECK

Type of Check	Signature(s)	Comments: (Including Reference to Check Document If Appropriate)
A. No check considered necessary		
B. Check vs. previous results/issues	[signature]	
C. Checked calculations made		
D. Checked computer input and/or output		
E. Computer Programs approved/qualified		
F. Performed independent audit		
G. Spot checked significant points	[signature]	
H. Reviewed methods used		
I. Reviewed results for reasonableness	[signature]	
J. Comparison with test data		
K. Reviewed vs. drawings		
L. Verified procedures		
M. Technical content reviewed	[signature]	
N. Management verification of adequate review by others		
O. Performed Lessons Learned Search		
P. Used Measurement Uncertainty Methods		
Q. Other Checks (Describe)		

3. CONCURRENCE REQUIREMENTS: Indicate signatures required by X:

___	ARP MANAGER	___	NCSG	___	FLUID DYNAM
___	NUCLEAR ENGINEERING	___	ADVANCED CONCEPTS	___	STRUC. ENGRG
___	REACTOR TH/MECH DESIGN	___	NOISE & ELEC. TECH.	___	DRAFTING
___	REACTOR EQUIPMENT	___	SHIELDING	___	QA
___	POWER PLANT MECHANICAL	___	REACTOR SAFETY	___	OTHER
___	POWER PLANT ELECTRICAL	___	TO	___	BETTIS
___	FINANCE	___	RSO	___	BPMI
___	NEW SHIP PROGRAMS	___	FSO	[signature]	ADMIN REVIEW
___	PROGRAM COORDINATION	___	MDO		

Cognizant Manager [signature]
(Must Be Subsection or Higher for External Letters)

4. AUTHORIZED CLASSIFIER: **Reviewed By:** [signature] **CLASSIFICATION:** UNCL

5. RELATED SUBJECTS:

UTRS Implication (Y/N)	___	Commitment Made (Y/N)	___	Commitment Complete (Y/N)	___
Safety Council Review (Y/N)	___	Design Basis Info. (Y/N)	___	UTRS Doc. #	___
		Design Review (Y/N)	___		

PRE-DECISIONAL – For Planning and Discussion Purposes Only

6. Distribution:

NR

D.I. Curtis, 08S (for information only)
J. D. Yoxtheimer, 08S
J.P. Mosquera, 08C
S.T. Bell, 08I
C.H. Oosterman, 08I
T.N. Roceheaver, 08I

PNR

J.F. Koury
J.A. Andes

SNR

D. Potts
D. Clapper
G.M. Millis
H. Miller

BETTIS

J.E. Hack*
M.N. Smith*
S.D. Harkness*
M.J. Zika
C.D. Eschelman*
D. Hagerty*
R.C. Jewart*
R. Baranwal
W. Ohlinger*
R. Buckman*
R.E. Gold*
E. Mader

KAPL

T.M. Angeliu
A. Guha*
M.J. Frederick
T.B. Schumaker*
Y. Ballout
S.A. Simonson
S. Frey*
R. Grossman*
J. Prybylowski
M. Wollman
J.A. Ashcroft*
J.K. Witter*
J.T. Ward*
W. Gideon*
K. Loomis*
D.F. McCoy*
H. Schwartzman*
C.F. Dempsey*
M. Chisano*
G.A. Newsome*
L.E. Kolaya*
B.C. Campbell*
A. Kolman*
D. Knorr*
M. Becker*
G.A. Young*
S. Sham*
SM File
ADSARS

* electronic copy only